iScience

CellPress
OPEN ACCESS

Article

CD32^{+}CD4^{+} memory T cells are enriched for total HIV-1 DNA in tissues from humanized mice

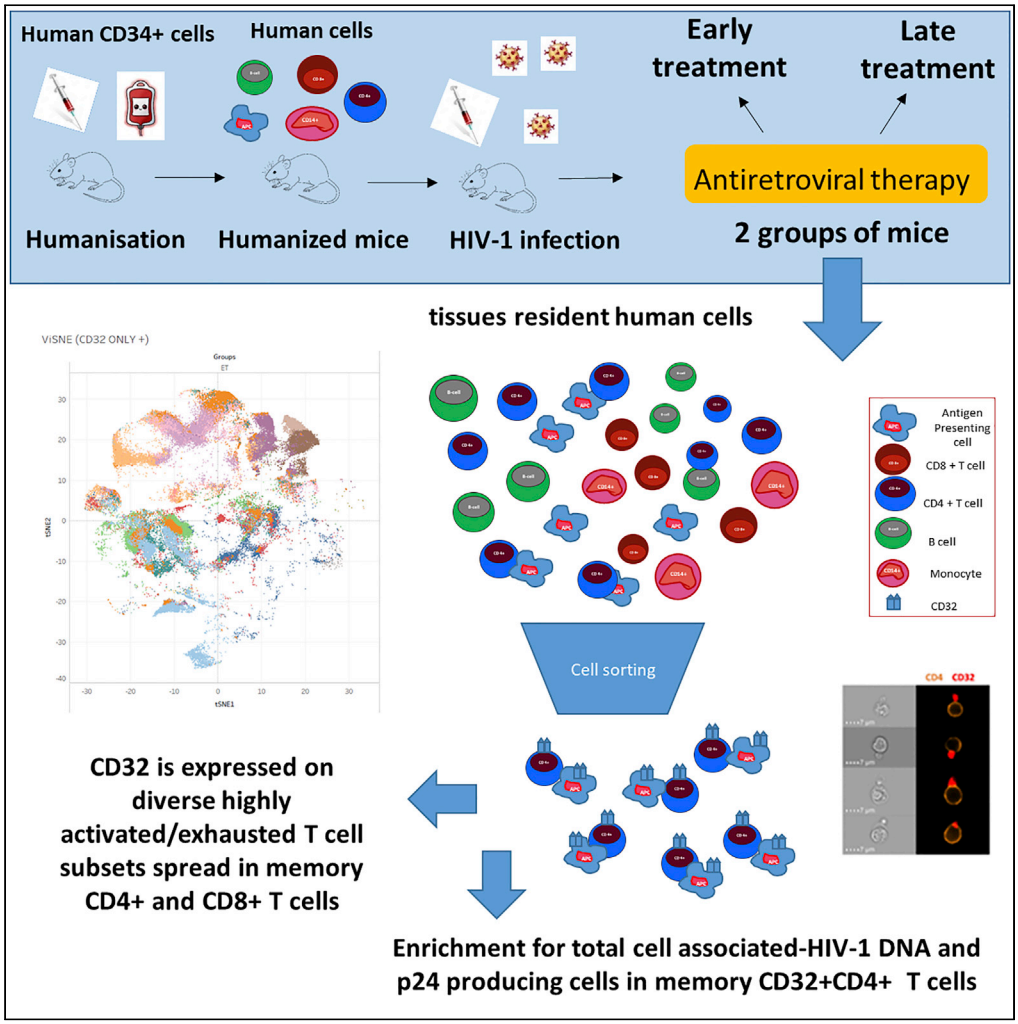

Philipp Adams, Virginie Fievez, Rafaëla Schober, ..., Michel Moutschen, Linos Vandekerckhove, Carole Seguin-Devaux

carole.devaux@lih.lu

HIGHLIGHTS

CD32 is rarely expressed in memory CD4^{+}T cells in humanized mice infected with HIV-1

Tissue-resident CD32^{+}CD4^{+} memory T cells are enriched for HIV-1 DNA but not for RNA

CD32^{+}CD4^{+} memory cells are enriched for translation-competent reservoirs

CD32 labels highly activated/exhausted memory T-cell subsets in tissues

Adams et al., iScience 24, 101881
January 22, 2021
https://doi.org/10.1016/j.isci.2020.101881

iScience

CellPress
OPEN ACCESS

Article

$CD32^+CD4^+$ memory T cells are enriched for total HIV-1 DNA in tissues from humanized mice

Philipp Adams,[1,2,3,8] Virginie Fievez,[1,8] Rafaëla Schober,[1] Mathieu Amand,[1] Gilles Iserentant,[1] Sofie Rutsaert,[4] Géraldine Dessilly,[5] Guido Vanham,[2,3] Fanny Hedin,[6] Antonio Cosma,[6] Michel Moutschen,[7] Linos Vandekerckhove,[4] and Carole Seguin-Devaux[1,9,*]

SUMMARY

CD32 has raised conflicting results as a putative marker of the HIV-1 reservoir. We measured CD32 expression in tissues from viremic and virally suppressed humanized mice treated relatively early or late after HIV-1 infection with combined antiretroviral therapy. CD32 was expressed in a small fraction of the memory $CD4^+$ T-cell subsets from different tissues in viremic and aviremic mice, regardless of treatment initiation time. $CD32^+$ memory $CD4^+$ T cells were enriched in cell-associated (CA) HIV-1 DNA but not in CA HIV-1 RNA as compared to the $CD32^-CD4^+$ fraction. Using multidimensional reduction analysis, several memory $CD4^+CD32^+$ T-cell clusters were identified expressing HLA-DR, TIGIT, or PD-1. Importantly, although tissue-resident $CD32^+CD4^+$ memory cells were enriched with translation-competent reservoirs, most of it was detected in memory $CD32^-CD4^+$ T cells. Our findings support that CD32 labels highly activated/exhausted memory $CD4^+$ T-cell subsets that contain only a small proportion of the translation-competent reservoir.

INTRODUCTION

The advent of combined antiretroviral therapy (cART) has dramatically improved the clinical care of HIV-1 infection. Since the START trial demonstrated that immediate initiation of cART is superior in reducing serious acquired immunodeficiency syndrome (AIDS)- and non-AIDS-related events (Lundgren et al., 2015), treatment guidelines advise to start therapy as early as possible (Panel on Antiretroviral Guidelines for Adults and Adolescents, 2017). Although beneficial in reduction of morbidities, early treatment started even during acute infection is not curative due to the establishment of long-lived viral reservoirs (Chun et al., 1998; Archin et al., 2012; Deng and Siliciano, 2014; Colby et al., 2018). Viral reservoirs, quantified by total HIV-1 DNA, are generally described as all cells infected with HIV-1, irrespective of their replication status or competence (Avettand-Fenoel et al., 2016). Viral persistence of replication-competent HIV-1 under cART, on a timescale of years, is however attributed to the latent portion of viral reservoirs. Therefore, using a practical definition (Eisele and Siliciano, 2012), latently infected cells that contain dormant but replication-competent provirus and are capable to resume viral production at a future time point represent the HIV-1 reservoir.

Latently infected cells have a half-life of 43.9 months, which makes them extremely resistant to antiretroviral therapy (ART). Therefore, discontinuation of treatment will, with great certainty, be followed by a viral rebound. The establishment of HIV-1 reservoirs occurs very rapidly upon primary infection. In simian immunodeficiency virus, reservoirs are found as early as three days post-infection in various tissues, even before virus detectability in circulation (Whitney et al., 2014). Likewise, in humans, initiation of cART during the acute phase of infection does not impede reservoir formation (Chun et al., 1998; Colby et al., 2018). Latent reservoirs are extremely stable with an estimated half-life of 43.9 months. This significantly hinders cART ability to eliminate HIV-1 within a patient's lifetime, with viral rebound highly likely to happen after treatment interruption (Siliciano et al., 2003b; Besson et al., 2014; Buzon et al., 2015; Crooks et al., 2015). The frequency of latently infected cells is very low (approximately 1 in 10^5-10^8 of $CD4^+$ T cells) (Finzi et al., 1997; Siliciano et al., 2003a; Strain et al., 2005), resulting in enormous technical challenges to precisely determine and study HIV-1 latency. Originally, the highest frequency of latently infected cells was thought to be localized in resting central memory $CD4^+$ T cells (Chomont et al., 2009; Descours et al., 2012; Sáez-

[1]Department of Infection and Immunity, Luxembourg Institute of Health, Esch-sur-Alzette 4354, Luxembourg

[2]Department of Biomedical and Clinical Sciences, Institute of Tropical Medicine, Antwerp 2000, Belgium

[3]Department of Biomedical Sciences, University of Antwerp, Antwerp 2000, Belgium

[4]HIV Cure Research Center, Department of Internal Medicine and Pediatrics, Ghent University, Ghent 9000, Belgium

[5]AIDS Reference Laboratory, Catholic University of Louvain, Brussels 1348, Belgium

[6]Quantitative Biology Unit, National Cytometry Platform, Luxembourg Institute of Health, Esch-sur-Alzette L-4354, Luxembourg

[7]Department of Infectious Diseases, University of Liège, CHU de Liège, Liège 4000, Belgium

[8]These authors contributed equally

[9]Lead Contact

*Correspondence: carole.devaux@lih.lu

https://doi.org/10.1016/j.isci.2020.101881

Cirión et al., 2013), but its heterogeneous dissemination over various $CD4^+$ T-cell memory subsets has been now recognized (Buzon et al., 2014; Banga et al., 2016; Zerbato et al., 2019; Kwon et al., 2020). In addition, the tissue distribution of reservoirs is diverse and poorly reflected by recirculating $CD4^+$ T cells in peripheral blood (Blum and Pabst, 2007; De Scheerder et al., 2019). Against this background, the characterization of cellular biomarkers of latently infected cells would enormously facilitate the development of strategies for their targeted depletion.

Various surface markers (CXCR3, CCR6, CD2, PD-1, LAG-3, TIGIT) were proposed to identify latently infected $CD4^+$ T cells but studies have not converged (Iglesias-Ussel et al., 2013; Anderson et al., 2014; Banga et al., 2018; Fromentin et al., 2016; Gosselin et al., 2017). The Fc-γ-RII receptor CD32 was recently proposed as a putative marker of cells highly enriched for total HIV-1 DNA and for replication-competent provirus (Descours et al., 2017). These findings have attracted a lot of attention but some recent works have relinquished inconclusive results (Abdel-Mohsen et al., 2018; Bertagnolli et al., 2018; Martin et al., 2018; Noto et al., 2018). $CD32^+$ $CD4^+$ T cells were shown to harbor a higher activation profile and to correlate with general immune activation. Overall, data from several patient cohorts did not substantiate the relevance of CD32 expression in latent HIV-1 reservoir probably due to the heterogeneity of cART initiation's timing, cART duration, and levels of immune activation. Recently, the different purity of $CD32^+CD4^+$ T cells across various studies was proposed as a possible explanation for these divergent findings (Abdel-Mohsen et al., 2018; Darcis et al., 2019). Furthermore, only few studies have scrutinized the role of CD32 in tissues (Noto et al., 2018; Cantero-Pérez et al., 2019; Thornhill et al., 2019).

Molecular mechanisms of HIV-1 latency have been mainly studied in cell lines, but these data have very limited relevance within clinical settings (Han et al., 2007; Van Lint, Bouchat and Marcello, 2013; Whitney and Brad Jones, 2018). Instead, humanized mice models have earned their place in HIV-1 research as versatile tools to study HIV-1 pathogenesis *in vivo* (Marsden and Zack, 2017). To date, cART treatment has reproduced the features of HIV-1 latency in these small animals (Marsden et al., 2017; Satheesan et al., 2018). The advantages of such models are the easy access to all anatomical sites and the precise control over timing and duration of treatment allowing a detailed understanding of HIV-1 latency under various conditions.

We have developed an HIV-1 latency model in humanized Nonobese diabetic/Severe Combined Immuno-Deficient gamma (NSG) mice to investigate the early establishment of the viral reservoir in untreated, early (one week after HIV-1 infection), and late treated mice (seven weeks after HIV-1 infection) with cART. Our study examined the expression of CD32 as a marker of viral reservoirs in memory CD4+T cells with capabilities of long-term persistence and its relationship to immune activation. Using a strict flow cytometry gating strategy, we show here that CD32 expression was low in $CD4^+$ T cells from different tissues in humanized mice treated early or late and was mostly due to the expression of the CD32a isoform. $CD32^+CD4^+$ memory T cells were enriched in cell-associated HIV-1 DNA (CA HIV-1 DNA) but not in cell-associated HIV-1 RNA (CA HIV-1 RNA), indicating HIV latency in these cells. $CD32^+CD4^+$ memory subsets were associated with their activation/exhaustion status under cART, and cluster analysis revealed that $CD32^+CD4^+$ memory cells are phenotypically related to cells expressing HLA-DR, PD-1, or TIGIT. Importantly, most of the p24 productive reservoir upon latency reversal was situated in the $CD32^-$ memory $CD4^+$ T cell fraction. Taken together, our data indicate that CD32 expression describes activated $CD4^+$ T-cell memory subsets enriched for proviral DNA independently of treatment initiation. Ultimately, we showed here that CD32 does not clearly label the translation-competent HIV-1 reservoir that needs to be eliminated in the perspective of HIV-1 cure.

RESULTS

Early cART treatment leads to faster viral suppression than late treatment in humanized mice

In this study, NSG mice were "humanized" with CD34+ hematopoietic stem cells over 24 weeks and then infected with HIV-1 JR-CSF Infectious Molecular Clone (pYK-JRCSF). One group was left untreated, a second group was treated early (one week after HIV-1 infection), and a third group was treated late (seven weeks after HIV-1 infection) (Figure 1).

In each group, oral treatment was maintained for eight weeks. As expected, in all conditions, a sharp increase of plasma HIV-1 RNA in the range of 10^4-10^5 copies per ml was detected during the first week after infection (Figure 2A). Subsequently, plasma viremia was strongly reduced within two weeks of either early

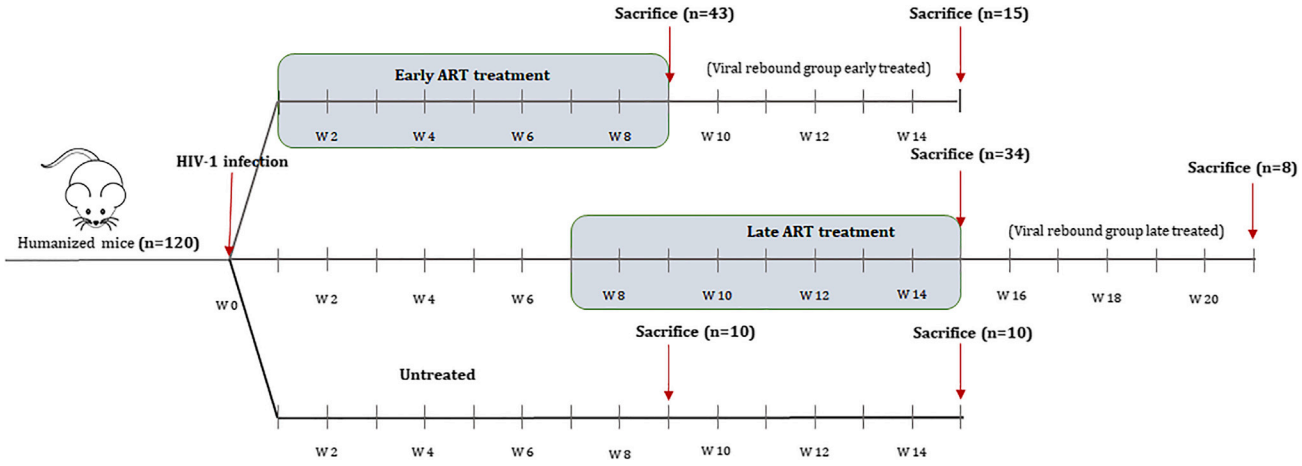

Figure 1. Design of the Study

One hundred twenty humanized NSG mice were infected with HIV-1 JRCSF. At week one post-infection, the cART regimen was initiated (n = 58) in the early treated group and sustained for two months. Late treatment was started at seven weeks post-infection (n = 42) and continued for two months. In each group, a number of animals were sacrificed at the end of treatment, corresponding to week nine for early treated (n = 43) and to week fifteen for late treated (n = 34) animals. The untreated group (n = 20) never received cART and was euthanized correspondingly to the sacrifices of both treatment groups (week nine for early treated and week fifteen for late treated mice). Viral rebound after treatment interruption was monitored for the remaining early (n = 15) and late treated (n = 8) animals for a duration of six weeks or longer if animals were not detectable for HIV-1 viral load.

or late treatment. Interestingly, early treatment led to a significantly quicker viral suppression (i.e. undetectability of the viral load) ($p < 0.0001$, Figure 2C). Conversely, the kinetics of viral rebound after treatment interruption were similar for both treatment groups (Figure 2D). Importantly, we observed that a portion of early treated mice rebounded only transiently (four out of fifteen or 26.7%) with "spontaneous" viral suppression up to six weeks after treatment cessation, whereas this "secondary control" phenomenon was not observed in the late treated group (Figures S1A and S1B). We measured HIV-1 RNA in the bone marrow, spleen, and lymph nodes of early treated mice as compared to untreated viremic mice after one week of HIV-1 infection. Viral loads were almost undetectable in the bone marrow of the treated mice, whereas some ongoing HIV-1 replication still occurs in the spleen and in the lymph nodes as shown by a detectable viral load in these two tissues (Figures S1C and S1D). Taken together, these observations indicate the establishment of replication-competent viral reservoirs within one week of infection in this model.

The immunological hallmark of HIV-1 infection is the depletion of $CD4^+$ T cells. As expected, we observed a rapid decline in circulating $CD4^+$ T cells upon infection. At week three post-infection, untreated mice lost around one third of their human $CD4^+$ T cells, whereas early treatment prevented $CD4^+$ T-cell loss (Figure 2B). Late treatment onset allowed a gradual recovery of $CD4^+$ T cells. At the endpoint (week sixteen), the late treated mice showed peripheral blood $CD4^+$ T-cell counts restored to similar levels when compared to the early treated mice (Figure 1). In agreement with our findings from peripheral blood (Figure 2B), the relative number of human $CD4^+$ T cells was also significantly increased by cART in the spleen for both treatment groups (Figures S2 and 2A). These data suggest recovery of the human $CD4^+$ T-cell compartment even after late cART onset in our model.

Total HIV-1 DNA and T-cell exhaustion are significantly reduced by early cART treatment

The stable persistence of provirus during therapy is a defining factor of HIV-1 latency. Therefore, we analyzed three different organ sites (bone marrow, lymph nodes, and spleen) for the presence of CA HIV-1 DNA by droplet digital Polymerase Chain Reaction (ddPCR), either at the end of cART treatment or corresponding time points for the non-treated animals (see experimental design in Figure 1). cART led to a significant reduction of CA HIV-1 DNA compared to the untreated control group (Figure 3A). Furthermore, early initiation of cART significantly reduced CA HIV-1 DNA as compared to late initiation in bone marrow (1.82 and 3.85 median $\log_{10}$ copies/million cells, respectively) and lymph nodes (2.45 and 3.7 median $\log_{10}$ copies/million cells, respectively), with a similar but non-significant trend observed in the spleen. These data underline that humanized mice mimic reservoir establishment and persistence during cART treatment similar to humans.

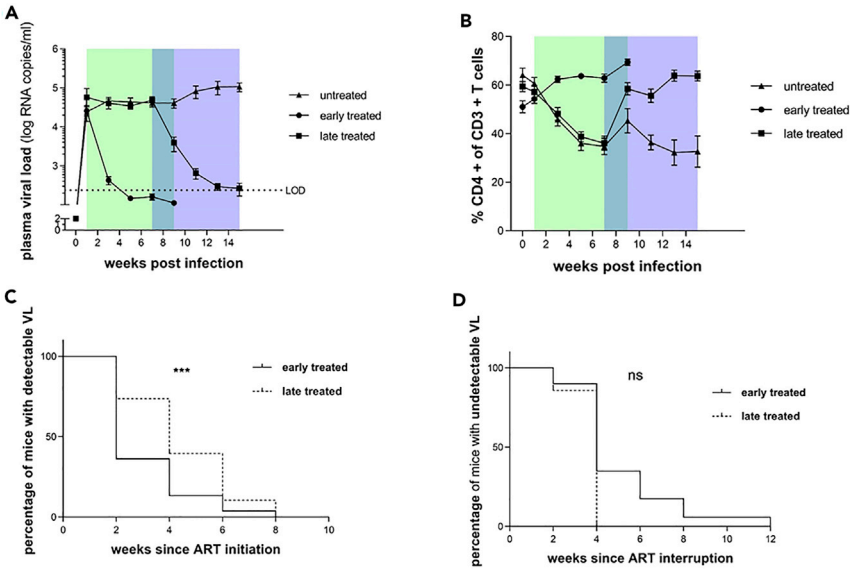

Figure 2. Early Treatment Significantly Decreased Time to Viral Suppression

(A and B) (A) Plasma viral load of early treated (n = 43), late treated (n = 34), and untreated (n = 20) mice and (B) percentage of $CD4^+$ T cells were determined every two weeks in peripheral blood. Background coloring of graphs highlights treatment periods: light green for early treatment, violet for late treatment, dark green is obtained by a two-week overlap (week seven to week nine) of early and late treatment periods (figure A and B).

(C and D) (C) Time to viral suppression (median two and four weeks, respectively) ($p < 0.0001$) and (D) viral rebound ($p = 0.107$) for the early and late group. Statistical analysis was executed using Mantel COX rank test. (***$p < 0.005$; ns, nonsignificant test $p > 0.05$).

Infection with HIV-1 induces not only loss of $CD4^+$ T cells in humans but also long-term alterations of the activation status in $CD4^+$ and $CD8^+$ T cells which persist during cART (Hazenberg et al., 2000; Hunt et al., 2003). In our humanized mice model, we assessed T-cell phenotypes in the tissues at the end of treatment and corresponding time points for untreated animals by flow cytometry. The expression of the exhaustion markers PD-1 and TIGIT was decreased by cART treatment on both CD4+ and CD8+ T cells, but the decrease was only significant between untreated and early treated groups (Figures 3B and 3C). Interestingly, the activation marker HLA-DR showed no difference among groups (Figures 3B and 3C). In addition, we observed a normalization of CD27 expression on CD4+ T cells by both treatment regimens (Figures S2B), suggesting a recovery in T-cell differentiation in our humanized mice model.

$CD32^+CD4^+$ memory T-cells do not contain T-B cell conjugates and harbor higher amounts of CA HIV-1 DNA but not of HIV-1 CA RNA

Next, we investigated the expression of CD32, a proposed marker of the HIV-1 reservoir. Given the previously reported technical difficulties to obtain pure $CD32^+CD4^+$ T cells (Martin et al., 2018; Osuna et al., 2018; Pérez et al., 2018), we applied an elaborated flow cytometry gating strategy to isolate $CD4^+$ memory T cells (defined as $CD45RA^-$) excluding doublets. To preclude contaminations by doublets, B cells or monocytes, strict singlet gating (on area versus width for forward and side scatter), as well as exclusion of CD19 and CD14 signals, were performed to analyze and sort $CD32^+CD4^+$ T cells by flow cytometry (Figure S3). The mean post-sorting purity of the $CD32^+CD4^+$ T cells was 98.8% of $CD4^+$ T-cell singlets (Figure S4). We observed also that human $CD4^+$ T cells contained a $CD32^{dim}$ population with low expression of CD32 in contrast to a $CD32^{bright}$ population expressed in $CD19^+$ B cells and T-B cell doublets or conjugates (Figure S5A). We next investigated whether T-B cell trogocytosis was involved as previously reported (Martin et al., 2018; Osuna et al., 2018; Thornhill et al., 2019) by using image cytometry on $CD32^+$ $CD4^+$ $CD45RA^-$ memory sorted T cells of humanized mice and of HIV-1-infected patients. $CD32^+CD4^+$ memory T cells contained no doublets, T-B cell conjugates, or B cell/monocyte contaminations (manual viewing of sorted cell images, data not shown). CD32 expression was localized in small, concentrated areas of $CD4^+$ T cells (Figures 4A and 4C) in contrast to sorted B cells on which CD32 was distributed homogeneously over the cell membrane (Figures 4B and 4D). Of note, no signal of CD19 or CD20 expression was detected on

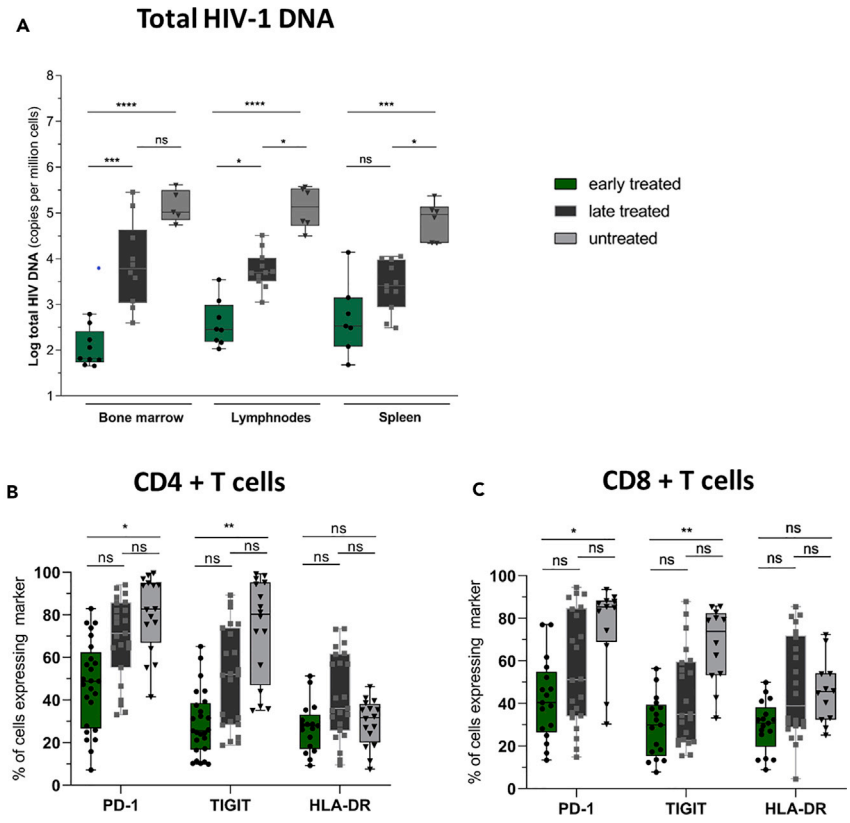

Figure 3. cART Significantly Decreased Total HIV-1 DNA in Peripheral Organs and HIV-1-Related Immune Exhaustion and Activation on Human T Cells

(A) Total HIV-1 DNA quantified from the bone marrow, lymph nodes, and spleen is represented for early treated (n = 9), late treated (n = 11), and untreated mice (n = 6). Percentages of cells expressing the respective markers PD-1, TIGIT, and HLA-DR on CD4+ T cells (B) and CD8+ T cells (C) extracted from the spleen at experimental endpoint (median age of nine months, eight weeks total cART duration for both treatment groups) are depicted for early treated mice (n = 17), late treated mice (n = 23), and untreated mice (n = 16). Statistical testing was performed using non-parametric Kruskal-Wallis tests with multiple comparison Dunn's correction. (*$p < 0.05$, **$p < 0.01$, ***$p < 0.005$, ***$p < 0.001$, ns, nonsignificant test, $p > 0.05$).

$CD32^+CD4^+$ T cells (Figures 4A and 4C). Importantly, overlay images emphasize that CD32 expression is rooted in small, non-$CD4^+$ T-cell compartments attached to $CD4^+$ T cells (Figures 4E and 4F). To explore if other cell types known to closely interact with CD4+ T cells might be the source of these CD32 expressing fragments attached to the CD4+ T cells, we used flow cytometry in peripheral blood mononuclear cells (PBMCs) of two HIV-1-infected patients treated with cART for at least two years and we did not exclude B or CD14+ cells as previously done. We detected different lineage markers coexpressed on CD32+ CD4+ T cells that could explain the origin of the attached fragments (potential trogocytosis): between 30 and 39% of HLADR (**H**uman **L**eukocyte **A**ntigen – **DR** isotype) + CD19+ B cells, around 1% of NK cells (CD4+CD16 + HLADR+), 4% of monocytes (all CD14+ cells), and up to 1% of dendritic cells (CD11c+). Around 7% of CD32+ CD4+ T cells were expressing HLA-DR, and this expression was not provided by CD19+ B cells, CD11c+, or CD16+ cells. Therefore, as we excluded B cells and monocytes in our strict flow cytometry strategy in this study, the fragments attached to the CD4+ T cells might come from other antigen-presenting cells (APCs) or NK cells. Furthermore, we measured the mRNA expression of CD32a and CD32b by real-time PCR in sorted $CD32^+CD4^+CD45RA^-$T cells and in a pool of $CD14^+$ and $CD19^+$ cells that were excluded by our flow cytometry gating strategy. $CD32^+$ $CD4^+$ $CD45RA^-$ memory T cells expressed mainly CD32a and low levels of CD32b mRNA, whereas both CD32a and CD32b mRNA were expressed in the pool of $CD14^+$ and $CD19^+$ cells (Table 1), confirming the exclusion of B cells in our purified $CD32^+CD4^+$ memory T cells.

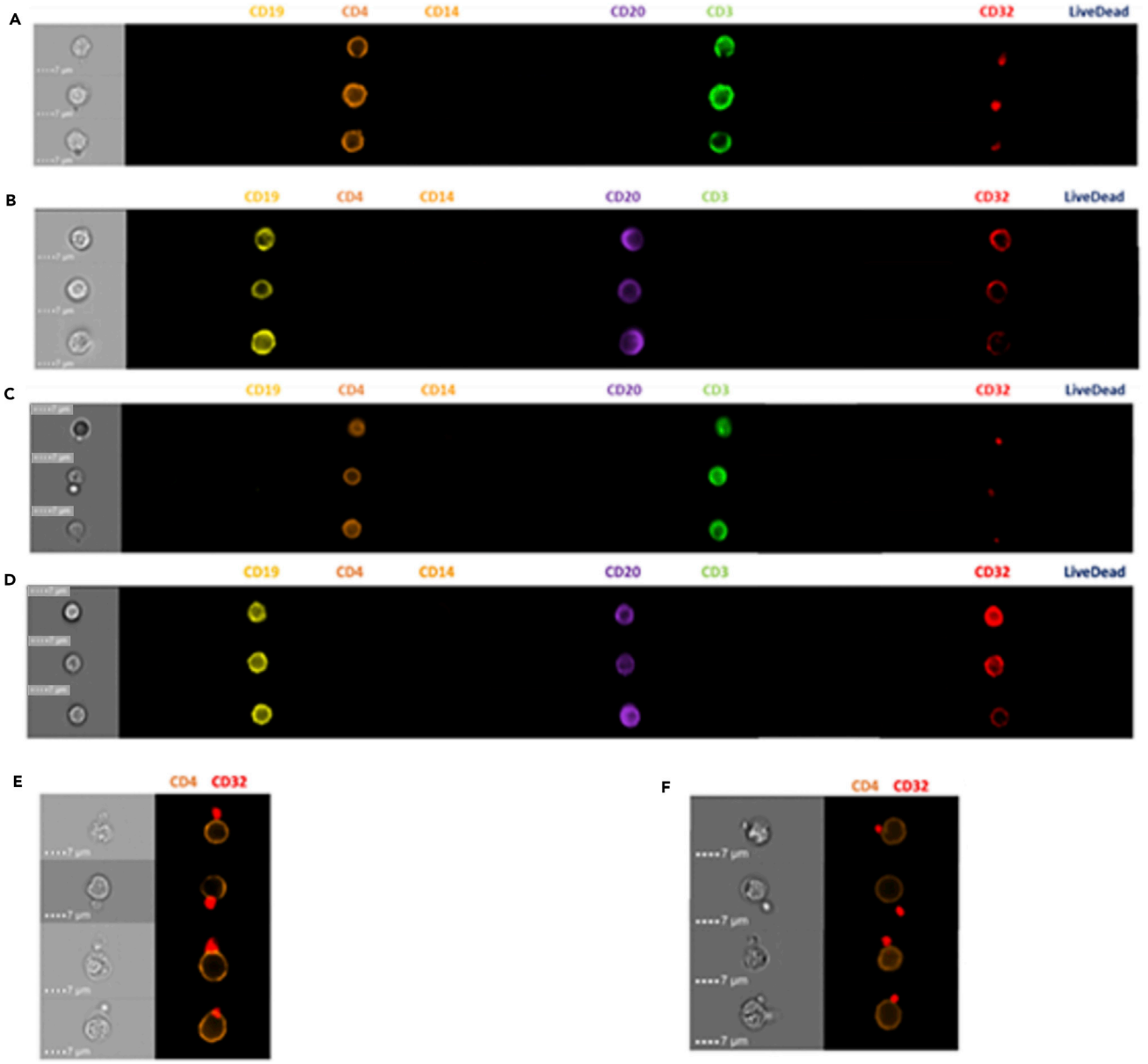

Figure 4. CD32 Is Expressed on Cell Fragments Attached to CD4$^+$ T Cells with No Signs of T-B Cell Trogocytosis

To assess whether the expression of CD32 on CD4$^+$ T cell comes from T cells or T-B cell conjugates, imaging flow cytometry was performed on sorted CD32$^+$CD4$^+$ T cells (A, C, E, and F) or sorted CD19$^+$ B cells (B and D) isolated from the spleen of cART suppressed HIV-1-infected humanized mice (A, B, E) or peripheral blood mononuclear cells (PBMCs) from cART suppressed HIV-1-infected patients (C, D, and F). Flow sorted B cells from humanized mice or patients were stained, acquired, and represented with the same settings and experimental procedures and,hence, serve as reference population with regard to CD32, CD19 ,and CD20 signal on images (B, D). Overlay shots of CD4 and CD32 signals of splenocytes from a humanized mouse (E) and of PBMCs from one HIV-1-infected patient (F).

When assessing the expression pattern of the memory CD32$^+$CD4$^+$ T cells in the different groups of mice, we found that overall CD32 cell surface expression did not differ substantially across various tissues nor between treatment groups (Figures S6A–S6D). Only lymph node T cells from healthy mice had significantly lower CD32 expression when compared to the untreated group (Figures S6 and 6D). Importantly, we did not find any difference during longitudinal sampling in the spleen (Figure S5B). To determine whether CD32 expressing cells were enriched for total CA HIV-1 DNA or RNA in cART-suppressed mice, CD32$^-$ and CD32$^+$ were flow sorted from the CD4$^+$ memory (i.e. CD45-) T cells. A sufficient quantity of CD32$^+$CD4$^+$ memory T cells were only obtained from the bone marrow and spleen. Memory

Mouse ID	BM	Spleen	Sorted cell fraction	Ct values			ΔCT value against GAPDH	
				CD32a	CD32b	GAPDH	CD32a	CD32b
S789	X		Pool of $CD19^+$ and $CD14^+$ cells	32,36	31,92	24,65	7,71	7,28
S803	X		Pool of $CD19^+$ and $CD14^+$ cells	28,86	30,4	21,76	7,1	8,63
S804	X		Pool of $CD19^+$ and $CD14^+$ cells	34,45	33,7	25,18	9,27	8,51
S789		x	Pool of $CD19^+$ and $CD14^+$ cells	34,51	32,91	27,92	9,59	4,98
S803		x	Pool of $CD19^+$ and $CD14^+$ cells	28,99	30,04	25,25	3,73	4,79
S804		x	Pool of $CD19^+$ and $CD14^+$ cells	32,35	30,9	26	6,35	4,9
S789	x		CD32-CD4+ memory T cells	36,58	37,14	25,07	11,51	12,7
S803	x		CD32-CD4+ memory T cells	36,67	36,09	25,36	11,3	10,73
S804	x		CD32-CD4+ memory T cells	36,23	37,61	25,97	10,26	11,64
S789		x	CD32-CD4+ memory T cells	39,48	38,31	27,73	11,75	10,58
S803		x	CD32-CD4+ memory T cells	36,75	36,79	25,37	11,38	11,41
S804		x	CD32-CD4+ memory T cells	36,67	36,69	24,81	11,86	11,88
S789, S803, and S804 pooled	x		CD32 + CD4+ memory T cells	32,14	36,72	26,69	5,45	10,02
S789, S803, and S804 pooled		x	CD32 + CD4+ memory T cells	34,21	38,82	28,74	5,47	10,08
PCR-negative controls				UND	UND	UND	NA	NA

Table 1. Gene expression of CD32a and CD32b mRNA isoforms of sorted $CD45RA^-CD32^-CD4^+$ T cells and a pool of $CD19^+$ and $CD14^+$ cells isolated from 3 single virally suppressed humanized mice (S789, S803, S804) and sorted $CD45RA^+CD32^+CD4^+$ T cells pooled from the 3 virally suppressed humanized mice

Results were analyzed against the GADPH Ct value. UND, undetectable; N/A, not available.

$CD32^+CD4^+$ T cells harbored significantly higher levels of HIV-1 DNA as compared to their CD32 negative counterparts (Figures 5A and 5B) in the spleen (4.35 vs 3.51 median $\log_{10}$ copies of HIV-1 DNA per million cells, respectively, $p < 0.01$) and in the bone marrow (4.42 vs 3.55 median $\log_{10}$ HIV-1 DNA copies per million cells, respectively, $p < 0.05$). Next, we quantified CA HIV-1 RNA but only 14 spleen-derived samples could be included due to low total RNA yield from $CD32^+CD4^+$ T cells. Although we used a limited set of sampling, we observed no difference for CA HIV-1 RNA between the $CD32^+CD4^+$ and the $CD32^-CD4^+$ memory subsets of the spleen (Figure 5C) (11.52 versus 45.16 median copies of CA RNA per million cells) for all mice with a detectable viral load.

CD32 is expressed on highly activated memory $CD4^+$ T cells and its level of expression does not correlate with the HIV-1 total DNA

Next, we assessed whether $CD32^+CD4^+$ T cells from tissue lymphocytes showed a particular activation/exhaustion profile as recently suggested (Badia et al., 2018). We found a significant upregulation of HLA-DR and PD-1 expression but not of the immune checkpoint marker TIGIT in $CD32^+CD4^+$ memory T cells (Figures 6A–6C), as compared to their $CD32^-$ counterparts. This trend was observed in both early ($p < 0.05$) and late treated mice ($p < 0.001$). We also measured the expression of the early and late activation markers CD69, HLA-DR, and CD38 (all combined in one channel) of the flow sorted $CD32^+$ and $CD32^-CD4^+$ memory T cells. A median of 80% $CD32^+CD4^+$ memory T cells expressed at least one of these activation markers as compared to a median of only 7% $CD32^-CD4^+$ memory T cells (Figure 6D). Moreover, the geometric mean fluorescence intensity (GMFI) of CD32 correlated moderately with the cumulated GMFI of the three activation markers (Spearman correlation, p value = 0.0004, r = 0.6872) (Figure 6E). In contrast, there was no correlation between CD32 expression and the total HIV-1 DNA content in $CD4^+$ T cells (data not shown, p value = 0.5809, r = −0.2167).

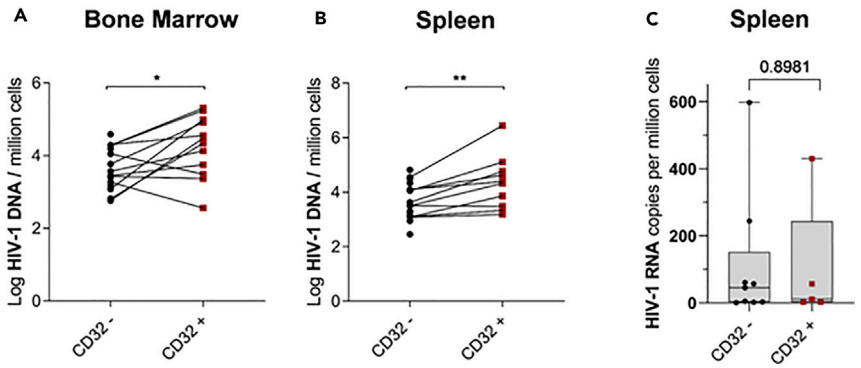

Figure 5. Total HIV-1 DNA Is Higher in CD32$^+$CD4$^+$ Memory T Cells in the Spleen and the Bone Marrow

Total HIV-1 DNA from flow sorted CD3$^+$CD4$^+$CD45RA$^-$ T cells according to CD32 expression in bone marrow (A) and spleen (B) in virally suppressed mice (mixed from early and late treatment conditions) (bone marrow n = 11, spleen n = 10) depicted as aligned dot plots of individual measurements (CD32- in black circles and CD32 + in red squares). The flow gating strategy is depicted in Figure S3. (C) HIV-1 CA RNA in flow sorted CD4$^+$ memory T cells (CD32$^-$ (n = 9) CD32$^+$ (n = 5)) from virally suppressed mice (mixed from early and late treatment conditions). Statistical testing was done using non-parametric paired Wilcoxon rank tests (A and B) or non-paired tests (C). Exact p values for HIV-1 DNA: bone marrow, 0.0278; spleen, 0.0039, (*p < 0.05. **p < 0.01).

We next performed multidimensional single-cell analysis using flow cytometry to investigate the activation/exhaustion co-expression patterns of the CD32$^+$CD4$^+$ memory T cells. CD32$^+$CD4$^+$ memory T cells were analyzed in untreated viremic mice (untreated [UT] mice, after four and eight weeks of HIV-1 infection) and in virally suppressed treated mice after four and eight weeks of cART treatment for both early (early treated [ET] mice) and late treated (late treated [LT] mice) groups. Co-expression of the markers was analyzed using the unsupervised algorithmic technique Flow Self-Organizing Map (FlowSOM). The clusters defined by FlowSOM (Figure 7A) were organized in a two-way hierarchical heatmap to determine their relationship (Figure 7B). Statistical analysis of the differential enrichment of clusters at week 4 and 8 revealed major changes in mice undergoing late treatment. Six clusters belonging to the central effector memory CD4 metacluster (metacluster number 8) showed an increase at week 8. The majority of these clusters expressed HLA-DR and in one we observed the expression of CD32 (cluster 6). Overall, clustering identified three CD4$^+$ T-cell populations harboring CD32 expression that showed a significant increase at week 8 in early treated mice (ET clusters 3, 11, 21) and one CD4$^+$CD32$^+$ cluster demonstrating a similar increase in late treated mice (LT clusters 6). Cluster 9 and 47 in LT mice were the unique CD4+CD32+ clusters showing a decrease at week 9. No significant changes were observed in UT mice. These memory CD4$^+$ clusters expressed either CD32^{dim} alone (ET cluster 21) or CD32^{dim} HLA-DR^{high} expression (ET cluster 3) or CD32^{dim} HLA-DR^{high} and PD-1^{low} expression (LT cluster 6) or CD32^{dim} HLA-DR^{dim} TIGIT^{high} PD-1^{dim} expression (ET cluster 11) or CD32^{high} HLA-DR^{dim} TIGIT^{dim} PD-1^{high} expression (LT cluster 9) (Figure 7B). Only one naive CD8$^+$CD32$^+$ cluster harboring HLA-DR^{high} expression was detected in CD8$^+$ T cells in late treated mice (LT cluster 47). These data showed the presence of phenotypically related activated or exhausted subsets in the memory CD4$^+$ CD32$^+$ T cells in the cART-treated mice when compared to their untreated counterpart. Overall, the expression of CD32 in these clusters was always associated with another activation (HLA-DR) or exhaustion marker (PD1, TIGIT), demonstrating that CD32 labeled a highly activated part of the memory CD4$^+$ T cells.

Tissue-resident memory CD32$^-$CD4$^+$ T cells contain most of the translation-competent virus producing p24

Finally, we sought to answer whether CD32$^+$CD4$^+$memory T cells contained the inducible translation-competent HIV-1 by assessing p24 production after phorbol myristate acetate (PMA)/ionomycin activation in the presence of raltegravir and lamivudine to prevent viral spread. Interestingly, more than 95% of p24 producing cells were detected in the CD32-negative fraction from the spleen in both viremic and virally suppressed mice (Figure 8B). Nevertheless, CD32$^+$CD4$^+$ memory T cells harbored a higher frequency of p24-positive cells when compared to CD32$^-$CD4$^+$ memory T cells suggesting a relative enrichment, as reported for total HIV-1 DNA (Figure 8C). Furthermore, we found higher levels of activation/exhaustion

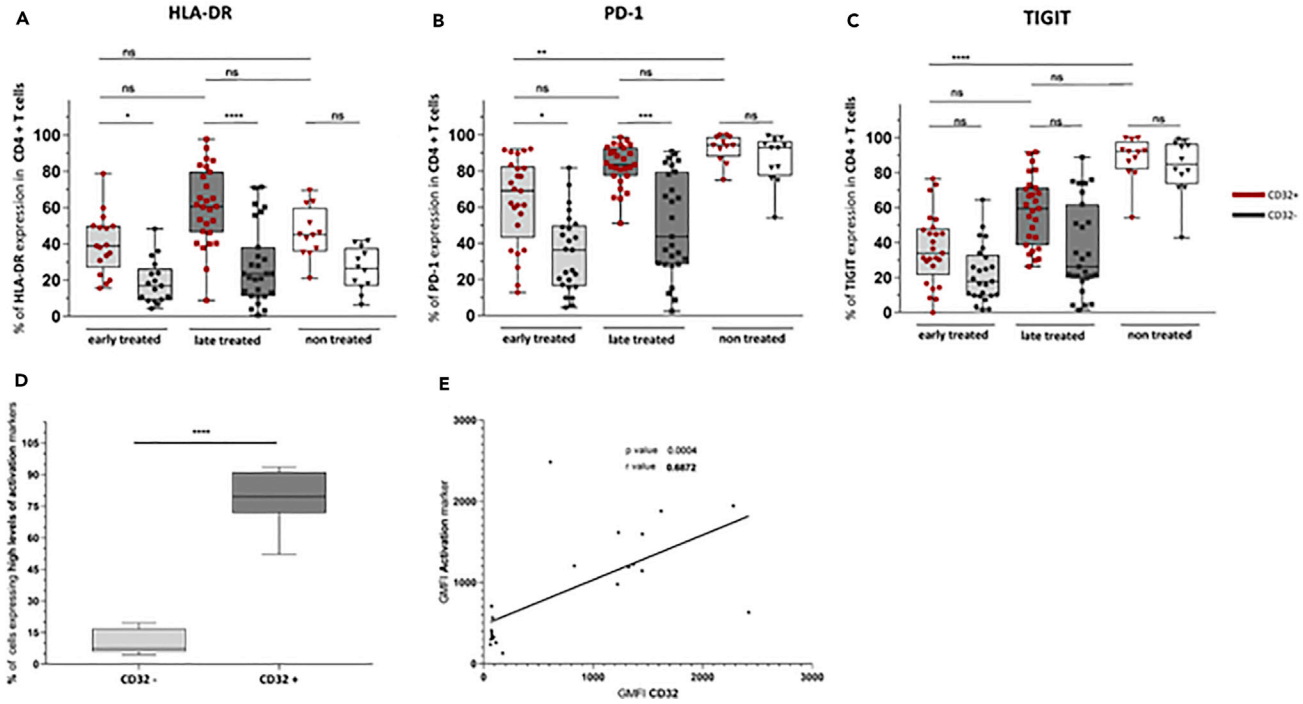

Figure 6. CD32 Expression Was Associated with High Expression Levels of Activation/Exhaustion Markers and Did Not Correlate with HIV-1 DNA

(A–C) Expression of HLA-DR (A), PD-1 (B), and TIGIT (C) in CD32-positive and negative $CD4^+$ memory T cells from the spleen.

(D) Expression level of three combined activation markers (HLA-DR, CD38, and CD69) in flow sorted $CD4^+$ memory T cells according to their CD32 expression. Geometric mean fluorescence intensity (GMFI) of activation markers plotted against the GMFI of CD32 from virally suppressed mice (mixed early and late treatment conditions).

(E) Spearman correlation with fitted linear regression line (p value: 0.0004, R value: 0.6872). Statistical testing by non-parametric Mann-Whitney or Kruskal-Wallis tests with multiple comparison Dunn's correction. Two-tailed spearman correlation (*$p < 0.05$, **$p < 0.01$, ***$p < 0.005$, ****$p < 0.001$, ns, nonsignificant test, $p > 0.05$).

markers on $CD32^+CD4^+$ memory T cells producing p24 than their $CD32^-$ counterpart, but this was significant only for PD1 (Figure 8D).

DISCUSSION

HIV-1 persists in a pool of latently infected CD4+ T cells, which constitutes a major barrier to curing HIV-1 (Katlama et al., 2013). Early studies found that this reservoir is mainly localized in $CD4^+$ resting T-cell memory subsets (Chomont et al., 2009) but recent evidence has substantiated on its wide spread distribution over various compartments of $CD4^+$ T cells (Buzon et al., 2014; Khoury et al., 2016; Hiener et al., 2017; Zerbato et al., 2019; Kwon et al., 2020). A number of strategies aiming at reducing the size of the HIV-1 reservoir are currently under investigation. Therefore, the discovery of a specific latently infected cell's marker could facilitate tailored interventions. CD32 was proposed as such by Descours et al. (Descours et al., 2017) but has been heavily debated ever since (Bruel and Schwartz, 2018; Darcis et al., 2019). Here, we scrutinized the relationship between the timing of ART initiation, T-cell immune activation/exhaustion, and reservoir characteristics with regard to CD32 expression in tissues from humanized mice in order to delineate its use as a surrogate marker of the viral reservoir.

Several groups have reported on humanized mice models of HIV-1 latency and their utility (Nischang et al., 2012; Halper-Stromberg et al., 2014; Iordanskiy et al., 2015; Satheesan et al., 2018; Llewellyn et al., 2019). We validated our humanized mice model of HIV-1 latency by first showing that the time to viral suppression was shortened by early cART treatment as compared to late therapy which is similar to clinical observation in humans (Ssebunya et al., 2017). Multiple studies have reported the benefits of early cART on immune activation. Persistent chronic infections trigger increased expression of immune checkpoints such as PD-1 and TIGIT on $CD4^+$ and $CD8^+$ T cells (Day et al., 2006; Trautmann et al., 2006), whereas cART

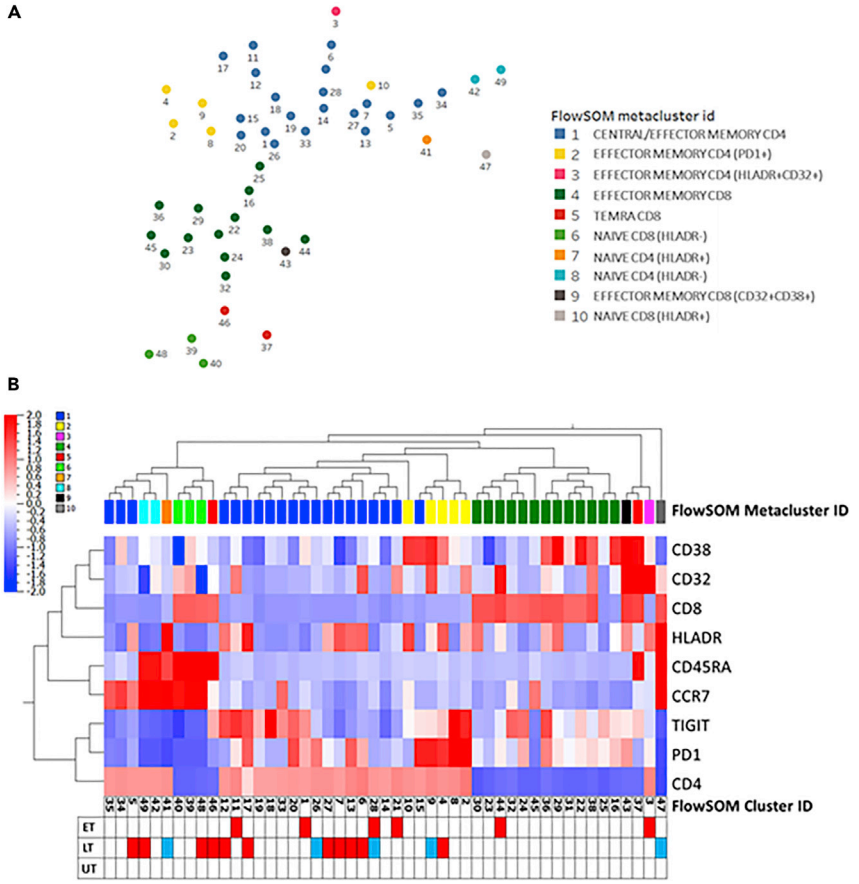

Figure 7. High-Dimensional Analyses Highlighted Different Activated/Exhausted Clusters Expressing CD32 in Memory CD4 T Cells from the Spleen of Early and Late Treated Mice with cART

(A) FlowSOM hierarchical tree colored according to metaclusters.

(B) Metaclusters were annotated according to the heatmap shown in. Two-way hierarchical clustering of the 49 clusters defined by FlowSOM and the median expression of the 9 markers indicated on the right of the heatmap. Median expression across the three groups of mice is shown. Three viremic untreated mice (untreated mice, UT)) were kept four weeks without treatment and four viremic mice were kept eight weeks; twenty-two mice were virally suppressed by receiving early cART treatment (n = 12, ET mice) or receiving late cART treatment (n = 10, LT). The clusters significantly different ($p < 0.05$) between four weeks and eight weeks of treatment are depicted on the bottom of the heatmap. A significant increase or decrease is indicated in red or cyan, respectively.

decreases PD-1 expression in parallel with reducing plasma VL after treatment onset (Cockerham et al., 2014b). In our study, we observed a consistent decline of PD-1 and TIGIT expression that was only significant by early cART initiation when compared to untreated mice. The T-cell activation marker HLA-DR was not significantly decreased by early or late cART regimen. Nevertheless, the recovery of total $CD4^+$ T-cell counts was rapid and successful in both treatment groups. These findings highlight that key aspects of HIV-1 pathogenesis and cART treatment are recapitulated in the presented model.

It is accepted that early cART effectively reduces the size of viral reservoirs and preserves the functionality of CD8 T cells, two conditions that might allow some individuals to achieve functional HIV-1 cure (Conway and Perelson, 2015). Our findings underline the impact of treatment initiation's timing on the level of total HIV-1 DNA spread in tissues as described in humans (Ananworanich et al., 2012; Laanani et al., 2015). Conversely, time to viral rebound did not differ between early and late treated conditions, similarly reported by two clinical studies that found also no prolonged control upon treatment cessation despite early ART initiation (Gianella et al., 2015; Colby et al., 2018). Consequently, it could be argued that total HIV-1 DNA, when sampled in tissues, is not a surrogate marker for time to viral rebound in contrast to human studies from peripheral blood (Azzoni et al., 2013; Williams et al., 2014). Importantly, we observed that a portion of early

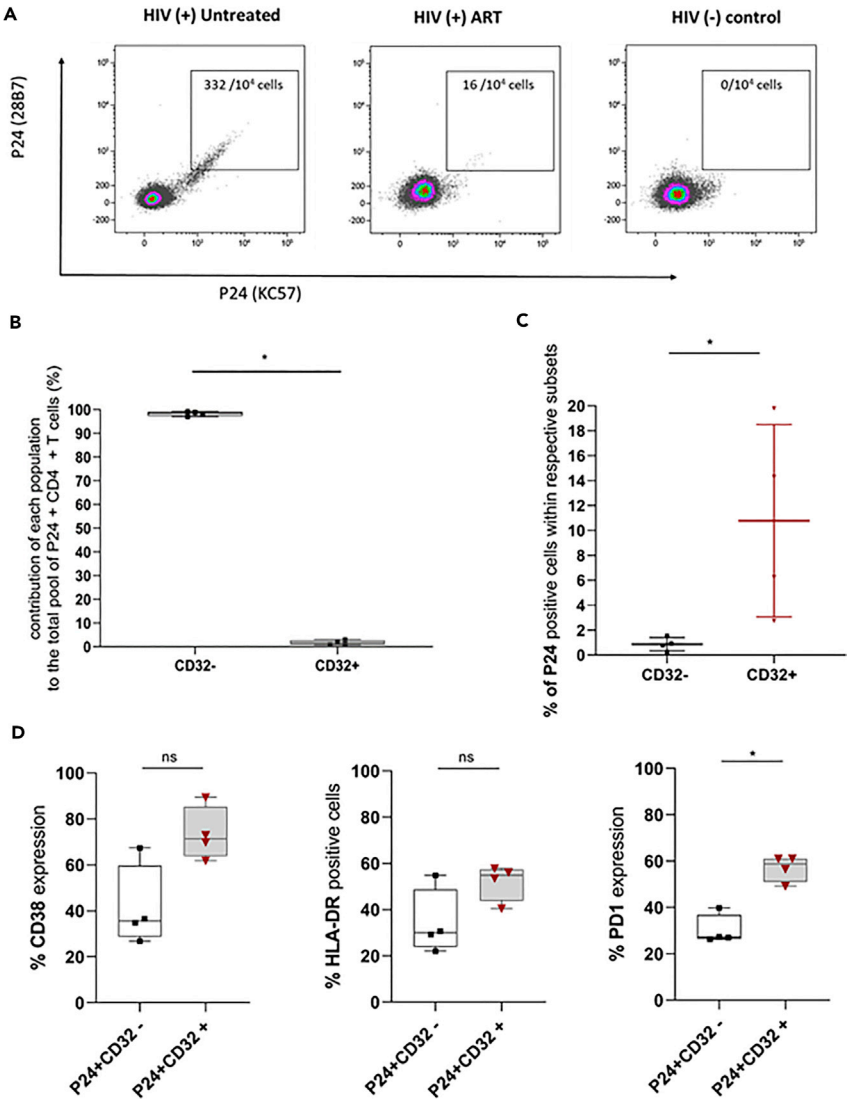

Figure 8. P24 Production after Latency Reversal Is Predominantly Found in CD32$^-$CD4$^+$ Memory T Cells and Not in the CD32$^+$ Fraction

(A) Representative fluorescence activated cell sorting (FACS) plots of p24 staining in an untreated viremic mouse after five weeks of HIV-1 infection and one ART-treated mouse, as well as a non-infected control mouse after PMA/ionomycin reactivation. The strict gating assured no false positive signal.

(B) Intracellular p24 staining after PMA/ionomycin activation in ART-treated animals (n = 4) revealed that the highest proportion of productive cells is CD32$^-$ and not CD32 $^+$.

(C) The frequency of p24 producing cells is higher within CD32$^+$CD4$^+$ memory T cells than in CD32$^-$ cells.

(D) Expression of HLA-DR, CD38, and PD-1 at the surface of the reactivated cells producing p24 from graph B. Statistics were performed using non-parametric testing. (*$p < 0.05$, ns, nonsignificant test, $p > 0.05$).

treated mice rebounded only transiently (26,67%) with subsequent "spontaneous" viral suppression, whereas this "secondary control" phenomenon was not observed in the late treated group. This suggests that early treatment increases the odds for delayed rebound, similar to a conclusion reached by the CHAMP cohort (Namazi et al., 2018) that found higher percentage of post-treatment control (PTC) in early treated individuals. The antiviral CD8$^+$ T-cell response could play a role during PTC, but this was not explored in greater detail because NSG mice lack antigen-specific T cells due to the absence of HLA-I presentation (Policicchio et al., 2016). Clearly, future studies should investigate the mechanisms of delayed rebound in this model. Taken together, our data showed however that the viral reservoir is already established and functional within one week after infection in most of the mice.

A number of cellular HIV-1 reservoir markers have been proposed over the last years. Among those markers the activation and immune checkpoint molecules HLA-DR, PD-1, TIGIT, but also CD32a (Cockerham et al., 2014a; Fromentin et al., 2016; Descours et al., 2017; Gosselin et al., 2017; Hogan et al., 2018). According to Descours et al., CD32a exhibited the promising trait to contain the replication-competent reservoir and to enrich for about 10^3 fold enrichment for total HIV-1 DNA (Descours et al., 2017). These results have been challenged by others, reporting either no (Abdel-Mohsen et al., 2018; Martin et al., 2018) or only marginal enrichment (Bertagnolli et al., 2018; Pérez et al., 2018), for both HIV-1 DNA and replication-competent proviruses. Such divergent findings were proposed to be due to technical tribulations during purification of $CD32^+CD4^+$ T cells (Darcis et al., 2019), as several studies showed that $CD32^+CD4^+$ T cells contained residual contamination by APCs which express high levels of CD32 (Martin et al., 2018; Osuna et al., 2018; Pérez et al., 2018; Thornhill et al., 2019). Therefore, we established a flow cytometry strategy with strict exclusion of B cells and monocytes (CD19 and CD14, respectively) as both cell types had been identified as sources for non-T-cell contamination before (Martin et al., 2018; Osuna et al., 2018). This approach enabled the identification of a $CD32^{dim}$ and not the $CD32^{high}$ population in a small fraction of $CD4^+$ T cells. Using imaging cytometry, in both humanized mice and in HIV-1-infected patients, we found that purified $CD32^+CD4^+$ T cells expressed CD32 on small, concentrated areas as previously reported by Osuna et al. (Osuna et al., 2018) but without co-localization of monocytes or B cell markers (CD19 or CD20), thus excluding B-cell trogocytosis. Still, we detected a polarized and concentrated localization of the CD32 protein on the membrane of $CD4^+$ T cells that could come from other APCs or NK cells. We detected CD32a mRNA expression on $CD4^+$ memory T cells and a weak expression of CD32b mRNA as well, whereas a pool of $CD19^+$ and $CD14^+$ population of B cells and monocytes expressed both CD32a and CD32b mRNA. This suggests endogeneous expression of CD32a by $CD4^+$ T cells similar to previous findings (Holgado et al., 2018; Darcis et al., 2020). However, the latter results have to be interpreted with caution as imaging cytometry data of ours and others (Osuna et al., 2018; Thornhill et al., 2019) unanimously challenge the origin of CD32 protein on $CD4^+$ T cells. We assume that CD32b mRNA might originate from the attached $CD32^+$ non-$CD4^+$ T-cell entities or from trogocytosis-positive T cells expressing higher level of activation markers, such as CD32a, due to more intensive T-cell/APC interaction. Taken together, we clearly identified a non-monocyte or non-B-cell-induced portion, potentially due to trogocytosis from other APC types or NK cells of $CD32^+CD4^+$ T cells or even from residual binding with platelets known to express CD32a. These findings are in line with a recent study working on highly pure $CD32^+CD4^+$ T cells (Darcis et al., 2020) and might advance the debate opened by many reports on the source for the CD32 signal on $CD4^+$ T cells (Martin et al., 2018; Osuna et al., 2018; Pérez et al., 2018; Thornhill et al., 2019). Ultimately, our results open new questions about the exact origin of the CD32 protein on $CD4^+$ T cells.

In our study, we further focused on CD32 expression in memory $CD4^+$ T cells ($CD45RA^-$) as this subset is comprises central and effector memory T cells which are well known to contain the highest frequencies of latently infected cells (Chomont et al., 2009; Bosque et al., 2011; Imamichi et al., 2014; Soriano-Sarabia et al., 2014; Murray et al., 2016). As compared to other studies, we included both resting (HLA-DR- or CD38- or CD69-) and non-resting (HLA-DR+ or CD38+ or CD69+) memory T cells. We found a significant increase of CD32 expression between HIV-1-infected and uninfected mice in human lymph nodes only as previously described (Bertagnolli et al., 2018). Importantly, a significant increase of about 0.85 $\log_{10}$ copies of CA HIV-1 DNA per millions cells in $CD32^+$ when compared to $CD32^-$ memory T cells was observed in virally suppressed mice. These findings are in agreement with results obtained from human lymph nodes (Noto et al., 2018) but not with data derived from peripheral blood of HIV-1-infected patients (Abdel-Mohsen et al., 2018; Badia et al., 2018; Osuna et al., 2018; Pérez et al., 2018) unless the $CD32^+$ cells underwent multiple, consecutive rounds of purification to exclude B cells, monocytes, and T-B cell doublets (Darcis et al., 2020). Despite CA HIV-1 DNA enrichment, there was no difference in CA HIV-1 RNA between $CD32^+$ and $CD32^-CD4^+$ memory T cells from the spleen, suggesting that CD32 labels cells with proviruses that are transcriptionally silent in tissues. However, the sample size of our data is limited because the total RNA yield from sorted subsets was low, and this represents a limitation of our study. Several studies from the lymph node and gut tissue reported the contrary (Abdel-Mohsen et al., 2018; Badia et al., 2018; Noto et al., 2018; Vasquez et al., 2019), but these findings are in accordance with a recent study from highly purified blood-derived lymphocytes (Darcis et al., 2020). Low transcription levels could be counterintuitive because we confirmed here, as others, that $CD32^+CD4^+$ T cells express HLA-DR activation marker. Nevertheless, activated subsets can indeed establish latent HIV-1 infection (Chavez, 2015; Lee et al., 2019).

CD32 is a low affinity receptor for the Fc portion of IgG (FcγR) which represents a link between humoral and cellular immunity and is highly expressed on myeloid cells and B cells. The functional role of CD32 on $CD4^+$ T cells is not well understood yet. However, it has been suggested that immune complexes might contribute to the continuation of chronic inflammatory responses by enhancing the activation of T cells through CD32 (Holgado et al., 2018) that might maintain persistence of the latent HIV-1 reservoir. Importantly, the expression of HLA-DR, CD38, and CD69 was strongly increased in $CD4^+CD32^+$ memory T cells from the tissues of cART-treated mice similar to recent studies from peripheral blood lymphocytes in humans (Badia et al., 2018; Wittner et al., 2018). Therefore, $CD32^+$ $CD4^+$ T cells might be more susceptible to HIV-1 infection because they are activated in a first place. The increased levels of HIV-1 co-receptors CXCR4 and CCR5 on $CD4^+CD32^+$ T cells on healthy individuals argue in favor of this concept (Hogan et al., 2018; Wittner et al., 2018). In addition, a recent study described tissue resident memory T cells from the cervical mucosa expressing CD32 as enriched for several proteins associated to HIV-1 susceptibility (Cantero-Pérez et al., 2019). $CD32^+CD4^+$ T cells could represent a pool of recently infected cells as drug penetration in tissues can be insufficient to suppress viral replication (Lorenzo-Redondo et al., 2016; Estes et al., 2017; Rothenberger et al., 2019). Accordingly, CD32 expression is induced upon infection with HIV-1 *in vitro* (Descours et al., 2017; Abdel-Mohsen et al., 2018; Badia et al., 2018). Furthermore, in human lymphoid and gut tissues, CD32 mRNA expression was associated with persistent HIV-1 mRNA replication (Hogan et al., 2018; Noto et al., 2018) which could indeed be explained by poor cART penetration unable to block residual HIV-1 replication. A relationship between active HIV-1 transcription and the CD32 gene has been already suggested (Abdel-Mohsen et al., 2018; Vasquez et al., 2019). Whether up-regulation of CD32 mRNA is a direct result of HIV-1 transcription or T-cell activation is still unknown. In this regard, our multidimensional reduction analysis revealed that $CD32^+CD4^+$ memory T cells have a high activation/exhaustion profile and clustered phenotypically with distinct activated/exhausted memory T-cell subsets expressing HLA-DR, PD-1, or TIGIT during suppressed viremia. This is in agreement with Badia et al. (2018) who has shown, following *ex vivo* HIV-1 infection in activated and resting cells or in PBMCs from HIV-1+ individuals, that CD32 expression is a marker of activation in a subset of CD4+ T cells both in uninfected controls and in HIV-1+ individuals. These authors state that establishment of HIV-1 latency may be the consequence of infection in CD4+T cells within a narrow window of time after activation. Thus, CD32 expression may signal a transition state to or from a fully susceptible phenotype. Our data provide further evidence that CD32 labels a highly activated/exhausted subset of memory $CD4^+$ T cells that might favor subsequently an HIV-1 enrichment in these cells.

Indispensable for the characterization of $CD4^+CD32^+$ T cells as latent HIV-1 reservoirs is to determine if they contain replication-competent virus and can resume to viral production. The current gold standard, the quantitative viral outgrowth assay (qVOA), requires large amounts of cells. Given the rarity of $CD32^+$ $CD4^+$ T cells in mice, we used intracellular p24 staining after *in vitro* latency reversal as reported previously. We found a relative enrichment of p24 production in $CD4^+CD32^+$ memory T cells similar in magnitude (about ten times) than the increase in CA HIV-1 DNA. However, overall $CD32^+CD4^+$ T cells constituted only a small portion of the total p24 inducible cellular reservoir (<5% of total p24 producing cells). Similar findings were reported in human lymph nodes (Abdel-Mohsen et al., 2018). Clearly, the presence of p24 alone, although produced in an advanced stage of the HIV-1 replication cycle, does not prove that the resulting viruses are correctly assembled, released, and infectious. Furthermore, a single round of stimulation with PMA/ionomycin for 24 hr only does not suffice to induce all replication-competent viruses (Ho et al., 2013; Laird et al., 2013). Unfortunately, there is currently no assay that can accurately activate the entire replication-competent fraction. Near full-length DNA sequencing does not take inducibility of viral gene transcription into account (Josefsson et al., 2013), and qVOA largely underestimates the replication-competent fraction (Ho et al., 2013). Taken together, our data underline that $CD4^+CD32^+$ memory T cells are enriched for p24 production after latency reversal but represent a small and negligible portion of the total inducible p24 producing cells.

Finally, the clinical relevance of the memory $CD32^+$ $CD4^+$ T cells as long-term viral reservoir remains difficult to estimate at this point in time. We observed a correlation of CD32 expression with the combined expression of all activation markers. Highly activated T cells are generally regarded as rather short lived (Chun et al., 2005; Noto et al., 2018) but their contribution to HIV-1 persistence is widely accepted (Hatano et al., 2013; Chavez, 2015; Deeks et al., 2016; Khoury et al., 2016; Lee et al., 2019). Consequently, for HIV-1 infection to persist, activated reservoirs are required for continous replenishment either by ongoing

viral replication (Martinez-Picado and Deeks, 2016) or by cellular proliferation (Chomont et al., 2009). Since CD32 was shown to promote immune activation in $CD4^+$ T cells *in vitro* (Holgado et al., 2018), it is tempting to speculate that CD32 itself could induce and maintain activation leading to preferential vulnerability to infection. The results of the cluster analysis reinforces this hypothesis by showing phenotypic similarities and a high number of clusters in the memory $CD32^+$ $CD4^+$ T cells as compared to the $CD32^+$ $CD8^+$ T cells. This in turn would question its role as a long-lived reservoir. Finally, there was a significant upregulation of PD-1 in $CD32^+$ vs $CD32^-$ cells producing the inducible translation-competent virus after PMA stimulation. Interestingly, Noto et al. have associated $CD32^+PD1^+CD4^+$ T cells from lymph nodes with the highest levels of HIV-1 transcription (Noto et al., 2018).

In conclusion, the present work highlights that tissue-resident $CD32^+CD4^+$ memory T cells represent different cellular subsets that are highly activated, enriched for total HIV-1 DNA, and produce P24 upon latency reversal. Despite a relative enrichment, $CD32^+CD4^+$ T cells form an overall negligible portion of the inducible P24 producing cells. Our findings support that CD32 expression is linked to immune activation in tissues which may explain the enrichment of CA HIV-1 DNA in $CD32^+CD4^+$ memory T cells. More distinctive markers to target the silent and replication-competent HIV-1 reservoir are still needed.

Limitations of the study

We acknowledge several limitations to our study. The limited life span of humanized mice allowed cART therapy for a maximum duration of eight weeks in our study design. This duration clearly differs from patient cohorts investigating HIV-1 latency after several years of suppressed viremia. Therefore, we cannot exclude the impact of short-lived reservoirs with decay rates above eight weeks (Palmer et al., 2011) and that the reservoir dynamics in CD32 + T cells derived from our latency model could be different than in patients with a longer treatment duration. This could potentially explain the lower relative enrichment in our humanized mice as compared to human PBMCs (Darcis et al., 2020). In addition, the quantity of blood available for longitudinal sampling and of human cells in tissues is also extremely limited in humanized mice. Lastly, PMA/ionomycin's activation used here to measure P24 producing cells might be able to induce only a fraction of the cells harboring translation-competent viruses in the humanized mice. A significant fraction of p24 producing cells does not also produce intact viral particles that are replication competent. Therefore, we induce probably only one part of the translation-competent virus in our study. However, the HIV-1 flow technique, by using 2 different P24 antibodies, provides a specific staining of the P24+ cells and allows us to compare accurately between CD32+ CD4+ memory T cells and their CD32-CD4+ counterpart, the translation-competent virus induced by PMA/ionomycin.

Resource availability

Lead contact

Further information and requests for resources should be directed to and will be fulfilled by the Lead Contact, Carole Devaux (caroledevaux@lih.lu).

Materials availability

The study did not generate any unique reagents.

Data and code availability

This published article includes all data sets generated or analyzed during this study.

METHODS

All methods can be found in the accompanying Transparent methods supplemental file.

SUPPLEMENTAL INFORMATION

Supplemental information can be found online at https://doi.org/10.1016/j.isci.2020.101881.

ACKNOWLEDGMENTS

The authors would like to thank Jean-Marc Plesseria, Charlène Verschueren, Jean-Yves Servais, Christine Lambert, and Quentin Etienne for their technical support. We thank Tuesday Lowndes for revising the manuscript for English language. The study (HIV latency) was funded by a research grant from the Ministry

of Research, the Fondation Recherche sur le SIDA of Luxembourg, an educational grant from ViiV Healthcare Benelux, and the FWO grant 1.8.020.09.N.00 (Linos L.V.). A.P. received a PhD AFR grant, F.V. a Mobility grant, and S.R. a PhD DTU PRIDE grant (Next-Immune) from The "Fonds National de la Recherche" in Luxembourg. R.S. received a strategic basic research fund of the Research Foundation – Flanders (FWO, 1S32916N) and V.L. a Collen-Francqui Research Professor Mandate.

AUTHOR CONTRIBUTIONS

A.P. and F.V. setup the HIV-1 latency model in humanized mice, designed experiments, performed and analyzed all experiments, drafted figures, and wrote the manuscript; S.R. performed experiments in humanized mice and measured viral loads; A.M. performed and designed experiments in humanized mice and drafted figures; I.G. performed flow cytometry, cell sorting, cell cultures, and Flow SOM analysis; R.S. performed ddPCR assays for the measurement of CA HIV-1 RNA and CA HIV-1 DNA; D.G. setup the viral load assay; V.G. analyzed and designed the experiments; C.A. designed and conducted the multidimensional reduction analysis; H.F. performed flow SOM and cluster analysis; M.M. setup the humanized mouse model of HIV-1 infection and provided cord blood cells; V.L. designed the ddPCR studies and analyzed the results; S.-D.C designed, analyzed the data, supervised the study, and wrote the manuscript. All authors participated in the preparation and editing of the manuscript.

DECLARATION OF INTERESTS

The authors declare that the research was conducted in the absence of any commercial or financial relationships that could be construed as a potential conflict of interest.

Received: March 26, 2020
Revised: September 4, 2020
Accepted: November 25, 2020
Published: January 22, 2021

REFERENCES

Abdel-Mohsen, M., Kuri-Cervantes, L., Grau-Exposito, J., Spivak, A.M., Nell, R.A., Tomescu, C., Vadrevu, S.K., Giron, L.B., Serra-Peinado, C., Genescà, M., Castellví, J., Wu, G., Del Rio Estrada, P.M., González-Navarro, M., Lynn, K., King, C.T., Vemula, S., Cox, K., Wan, Y., Li, Q., Mounzer, K., Kostman, J., Frank, I., Paiardini, M., Hazuda, D., Reyes-Terán, G., Richman, D., Howell, B., Tebas, P., Martinez-Picado, J., Planelles, V., Buzon, M.J., Betts, M.R., and Montaner, L.J. (2018). CD32 is expressed on cells with transcriptionally active HIV but does not enrich for HIV DNA in resting T cells. Sci. Transl Med. *10*, eaar6759.

Ananworanich, J., Schuetz, A., Vandergeeten, C., Sereti, I., de Souza, M., Rerknimitr, R., Dewar, R., Marovich, M., van Griensven, F., Sekaly, R., et al. (2012). Impact of multi-targeted antiretroviral treatment on gut t cell depletion and HIV reservoir seeding during acute hiv infection. PLoS One *7*, e33948.

Anderson, J.L., Khoury, G., Fromentin, R., Solomon, A., Chomont, N., Sinclair, E., Milush, J.M., Hartogensis, W., Bacchetti, P., Roche, M., et al. (2020). Human Immunodeficiency Virus (HIV)-Infected CCR6+ rectal CD4+ T cells and HIV Persistence on antiretroviral therapy. J. Infect. Dis. *221*, 744–755.

Archin, N.M., Vaidya, N.V., Kuruc, J.D., Liberty, A.L., Wiegand, A., Kearney, M.F., Cohen, M.S., Coffin, J.M., Bosch, R.J., Gay, C.L., et al. (2012). Immediate antiviral therapy appears to restrict resting CD4+ cell HIV-1 infection without accelerating the decay of latent infection. PNAS *109*, 9523–9528.

Avettand-Fenoel, V., Hocqueloux, L., Ghosn, J., Cheret, A., Frange, P., Melard, A., Viard, J.P., and Rouzioux, C. (2016). Total HIV-1 DNA, a marker of viral reservoir dynamics with clinical implications. Clin. Microbiol. Rev. *29*, 859–880.

Azzoni, L., Foulkes, A.S., Papasavvas, E., Mexas, A.M., Lynn, K.M., Mounzer, K., Tebas, P., Jacobson, J.M., Frank, I., Busch, M.P., et al. (2013). Pegylated interferon alfa-2a monotherapy results in suppression of HIV type 1 replication and decreased cell-associated HIV DNA integration. J. Infect. Dis. *207*, 213.

Badia, R., Ballana, E., Castellví, M., García-Vidal, E., Pujantell, M., Clotet, B., Prado, J.G., Puig, J., Martínez, M.A., Riveira-Muñoz, E., et al. (2018). CD32 expression is associated to T-cell activation and is not a marker of the HIV-1 reservoir. Nat. Comm. *9*, 2739.

Banga, R., Procopio, F.A., Noto, A., Pollakis, G., Cavassini, M., Ohmiti, K., Corpataux, J.M., de Leval, L., Pantaleo, G., and Perreau, M. (2016). PD-1(+) and follicular helper T cells are responsible for persistent HIV-1 transcription in treated aviremic individuals. Nat. Med. *22*, 754.

Banga, R., Procopio, F.A., Ruggiero, A., Noto, A., Ohmiti, K., Cavassini, M., Corpataux, J.M., Paxton, W.A., Pollakis, G., and Perreau, M. (2018). Blood CXCR3+ CD4 T cells are enriched in inducible replication competent HIV in aviremic antiretroviral therapy-treated individuals. Front. Immunol. *9*, 144.

Bertagnolli, L.N., White, J.A., Simonetti, F.R., Beg, S.A., Lai, J., Tomescu, C., Murray, A.J., Antar, A.A.R., Zhang, H., Margolick, J.B., et al. (2018). The role of CD32 during HIV-1 infection. Nature *7723*, E17–E19.

Besson, G.J., Lalama, C.M., Bosch, R.J., Gandhi, R.T., Bedison, M.A., Aga, E., Riddler, S.A., McMahon, D.K., Hong, F., and Mellors, J.W. (2014). HIV-1 DNA decay dynamics in blood during more than a decade of suppressive antiretroviral therapy. Clin. Infect. Dis. *59*, 1312–1321.

Blum, K.S., and Pabst, R. (2007). Lymphocyte numbers and subsets in the human blood. Do they mirror the situation in all organs? Immunol. Lett. *108*, 45.

Bosque, A., Famiglietti, M., Weyrich, A.S., Goulston, C., and Planelles, V. (2011). Homeostatic proliferation fails to efficiently reactivate HIV-1 latently infected central memory CD4+ T cells. Plos Pathog. *7*, e1002288.

Bruel, T., and Schwartz, O. (2018). Markers of the HIV-1 reservoir: facts and controversies. Curr. Opin. HIV AIDS *13*, 383–388.

Buzon, M.J., Sun, H., Li, C., Shaw, A., Seiss, K., Ouyang, Z., Martin-Gayo, E., Leng, J., Henrich, T.J., Li, J.Z., et al. (2014). HIV-1 persistence in CD4+ T cells with stem cell-like properties. Nat. Med. *20*, 139.

Buzon, M.J., Martin-Gayo, E., Pereyra, F., Ouyang, Z., Sun, H., Li, J.Z., Piovoso, M., Shaw, A., Dalmau, J., Zangger, N., et al. (2015). Long-term antiretroviral treatment initiated at primary HIV-1 infection affects the size, composition, and decay

kinetics of the reservoir of HIV-1-infected CD4 T cells. J. Virol. *88*, 10056–10065.

Cantero-Pérez, J., Grau-Expósito, J., Serra-Peinado, C., Rosero, D.A., Luque-Ballesteros, L., Astorga-Gamaza, A., Castellví, J., Sanhueza, T., Tapia, G., Lloveras, B., et al. (2019). Resident memory T cells are a cellular reservoir for HIV in the cervical mucosa. Nat. Commun. *10*, 473.

Chavez, L., Calvanese, V., and Verdin, E. (2015). HIV latency is established directly and early in both resting and activated primary CD4 T cells. PLoS Pathog. *11*, e1004955.

Chomont, N., El-Far, M., Ancuta, P., Trautmann, L., Procopio, F.A., Yassine-Diab, B., Boucher, G., Boulassel, M.R., Ghattas, G., Brenchley, J.M., et al. (2009). HIV reservoir size and persistence are driven by T cell survival and homeostatic proliferation. Nat. Med. *15*, 893–900.

Chun, T.W., Engel, D., Berrey, M.M., Shea, T., Corey, L., and Fauci, A.S. (1998). Early establishment of a pool of latently infected, resting CD4+ T cells during primary HIV-1 infection. Proc. Natl. Acad. Sci. USA *95*, 8869–8873.

Chun, T.W., Nickle, D.C., Justement, J.S., Large, D., Semerjian, A., Curlin, M.E., O'Shea, M.A., Hallahan, C.W., Daucher, M., Ward, D.J., et al. (2005). HIV-infected individuals receiving effective antiviral therapy for extended periods of time continually replenish their viral reservoir. J. Clin. Invest. *115*, 3250.

Cockerham, L.R., Siliciano, J.D., Sinclair, E., O'Doherty, U., Palmer, S., Yukl, S.A., Strain, M.C., Chomont, N., Hecht, F.M., Siliciano, R.F., et al. (2014a). CD4+ and CD8+ T cell activation are associated with HIV DNA in resting CD4+ T cells. PLoS ONE *9*, e110731.

Cockerham, L.R., Jain, V., Sinclair, E., Glidden, D.V., Hartogenesis, W., Hatano, H., Hunt, P.W., Martin, J.N., Pilcher, C.D., Sekaly, R., et al. (2014b). Programmed death-1 expression on $CD4^+$ and $CD8^+$ T cells in treated and untreated HIV disease. AIDS *28*, 1749–1758.

Colby, D.J., Trautmann, L., Pinyakorn, S., Leyre, L., Pagliuzza, A., Kroon, E., Rolland, M., Takata, H., Buranapraditkun, S., Intasan, J., et al. (2018). Rapid HIV RNA rebound after antiretroviral treatment interruption in persons durably suppressed in Fiebig I acute HIV infection. Nat. Med. *24*, 923–926.

Conway, J.M., and Perelson, A.S. (2015). Post-treatment control of HIV infection. Proc. Natl. Acad. Sci. USA *112*, 5467.

Crooks, A.M., Bateson, R., Cope, A.B., Dahl, N.P., Griggs, M.K., Kuruc, J.D., Gay, C.L., Eron, J.J., Margolis, D.M., Bosch, R.J., and Archin, N.M. (2015). Precise quantitation of the latent HIV-1 reservoir: implications for eradication strategies. J. Infect. Dis. *212*, 1361.

Darcis, G., Kootstra, N.A., Hooibrink, B., van Montfort, T., Maurer, I., Groen, K., Jurriaans, S., Bakker, M., van Lint, C., Berkhout, B., and Pasternak, A.O. (2020). CD32+CD4+ T cells are highly enriched for HIV DNA and can support transcriptional latency. Cell Rep *30*, 2284-e3.

Darcis, G., Berkhout, B., and Pasternak, A.O. (2019). The quest for cellular markers of HIV reservoirs: any color you like. Front. Immunol. *10*, 2251.

Day, C.L., Kaufmann, D.E., Kiepiela, P., Brown, J.A., Moodley, E.S., Reddy, S., Mackey, E.W., Miller, J.D., Leslie, A.J., DePierres, C., et al. (2006). PD-1 expression on HIV-specific T cells is associated with T-cell exhaustion and disease progression. Nature *443*, 350–354.

Deeks, S.G., Lewin, S.R., Ross, A.L., Ananworanich, J., Benkirane, M., Cannon, P., Chomont, N., Douek, D., Lifson, J.D., Lo, Y.R., et al. (2016). International AIDS Society global scientific strategy: towards an HIV cure 2016. Nat. Med. *22*, 839.

Deng, K., and Siliciano, R.F. (2014). HIV: early treatment may not be early enough. Nature *512*, 35–36.

Descours, B., Avettand-Fenoel, V., Blanc, C., Samri, A., Mélard, A., Supervie, V., Theodorou, I., Carcelain, G., Rouzioux, C., and Autran, B. (2012). Immune responses driven by protective human leukocyte antigen alleles from long-term nonprogressors are associated with low HIV reservoir in central memory CD4 T cells. Clin. Infect. Dis. *54*, 1495–1503.

Descours, B., Petitjean, G., López-Zaragoza, J.L., Bruel, T., Raffel, R., Psomas, C., Reynes, J., Lacabaratz, C., Levy, Y., Schwartz, O., et al. (2017). CD32a is a marker of a CD4 T-cell HIV reservoir harbouring replication-competent proviruses. Nature *543*, 564–567.

Eisele, E., and Siliciano, R.F. (2012). Redefining the viral reservoirs that prevent HIV-1 eradication. Immunity *37*, 377–388.

Estes, J.D., Kityo, C., Ssali, F., Swainson, L., Makamdop, K.N., Del Prete, G.Q., Deeks, S.G., Luciw, P.A., Chipman, J.G., Beilman, G.J., et al. (2017). Defining total-body AIDS-virus burden with implications for curative strategies. Nat. Med. *23*, 1271.

Finzi, D., Hermankova, M., Pierson, T., Carruth, L.M., Buck, C., Chaisson, R.E., Quinn, T.C., Chadwick, K., Margolick, J., Brookmeyer, R., et al. (1997). Identification of a reservoir for HIV-1 in patients on highly active antiretroviral therapy. Science *278*, 1295.

Fromentin, R., Bakeman, W., Lawani, M.B., Khoury, G., Hartogensis, W., DaFonseca, S., Killian, M., Epling, L., Hoh, R., Sinclair, E., et al. (2016). CD4+ T cells expressing PD-1, TIGIT and LAG-3 contribute to HIV persistence during ART. Plos Pathog. *12*, e1005761.

Gianella, S., Anderson, C.M., Richman, D.D., Smith, D.M., and Little, S.J. (2015). No evidence of posttreatment control after early initiation of antiretroviral therapy. AIDS *29*, 2093.

Gosselin, A., Wiche Salinas, T.R., Planas, D., Wacleche, V.S., Zhang, Y., Fromentin, R., Chomont, N., Cohen, É.A., Shacklett, B., Mehraj, V., et al. (2017). HIV persists in CCR6+CD4+ T cells from colon and blood during antiretroviral therapy. AIDS *31*, 35–48.

Halper-Stromberg, A., Lu, C.L., Klein, F., Horwitz, J.A., Bournazos, S., Nogueira, L., Eisenreich, T.R., Liu, C., Gazumyan, A., Schaefer, U., et al. (2014). Broadly neutralizing antibodies and viral inducers decrease rebound from HIV-1 latent reservoirs in humanized mice. Cell *158*, 989.

Han, Y., Wind-Rotolo, M., Yang, H.C., Siliciano, J.D., and Siliciano, R.F. (2007). Experimental approaches to the study of HIV-1 latency. Nat. Rev. Microbiol. *5*, 95–106.

Hatano, H., Jain, V., Hunt, P.W., Lee, T.H., Sinclair, E., Do, T.D., Hoh, R., Martin, J.N., McCune, J.M., Hecht, F., et al. (2013). Cell-based measures of viral persistence are associated with immune activation and programmed cell death protein 1 (PD-1)-expressing CD4+ T cells. J. Infect. Dis. *208*, 50.

Hazenberg, M.D., Stuart, J.W., Otto, S.A., Borleffs, J.C., Boucher, C.A., de Boer, R.J., Miedema, F., and Hamann, D. (2000). T-cell division in human immunodeficiency virus (HIV)-1 infection is mainly due to immune activation: a longitudinal analysis in patients before and during highly active antiretroviral therapy (HAART). Blood *95*, 249.

Hiener, B., Horsburgh, B.A., Eden, J.-S., Barton, K., Schlub, T.E., Lee, E., von Stockenstrom, S., Odevall, L., Milush, J.M., Liegler, T., et al. (2017). Identification of genetically intact HIV-1 proviruses in specific CD4+ T cells from effectively treated participants. Cell Rep. *21*, 813–822.

Ho, Y.C., Shan, L., Hosmane, N.N., Wang, J., Laskey, S.B., Rosenbloom, D.I., Lai, J., Blankson, J.N., Siliciano, J.D., and Siliciano, R.F. (2013). Replication-competent noninduced proviruses in the latent reservoir increase barrier to HIV-1 cure. Cell *155*, 540.

Hogan, L.E., Vasquez, J., Hobbs, K.S., Hanhauser, E., Aguilar-Rodriguez, B., Hussien, R., Thanh, C., Gibson, E.A., Carvidi, A.B., Smith, L.C.B., et al. (2018). Increased HIV-1 transcriptional activity and infectious burden in peripheral blood and gut-associated CD4+ T cells expressing CD30. Plos Pathog. *14*, e1006856.

Holgado, M.P., Sananez, I., Raiden, S., Geffner, J.R., and Arruvito, L. (2018). CD32 Ligation Promotes the Activation of CD4. Front. Immunol. *9*, 2814.

Hunt, P.W., Martin, J.N., Sinclair, E., Bredt, B., Hagos, E., Lampiris, H., and Deeks, S.G. (2003). T cell activation is associated with lower CD4+ T cell gains in human immunodeficiency virus-infected patients with sustained viral suppression during antiretroviral therapy. J. Infect. Dis. *187*, 1534.

Iglesias-Ussel, M., Vandergeeten, C., Marchionni, L., Chomont, N., and Romerio, F. (2013). High levels of CD2 expression identify HIV-1 latently infected resting memory CD4+ T cells in virally suppressed subjects. J. Virol. *87*, 9148.

Imamichi, H., Natarajan, V., Adelsberger, J.W., Rehm, C.A., Lempicki, R.A., Das, B., Hazen, A., Imamichi, T., and Lane, H.C. (2014). Lifespan of effector memory CD4+ T cells determined by replication-incompetent integrated HIV-1 provirus. AIDS *28*, 1091.

Iordanskiy, S., Van Duyne, R., Sampey, G.C., Woodson, C.M., Fry, K., Saifuddin, M., Guo, J., Wu, Y., Romerio, F., and Kashanchi, F. (2015). Therapeutic doses of irradiation activate viral

transcription and induce apoptosis in HIV-1 infected cells. Virology *485*, 1.

Josefsson, L., Palmer, S., Faria, N.R., Lemey, P., Casazza, J., Ambrozak, D., Kearney, M., Shao, W., Kottilil, S., Sneller, M., et al. (2013). Single cell analysis of lymph node tissue from HIV-1 infected patients reveals that the majority of CD4+ T-cells contain one HIV-1 DNA molecule. Plos Pathog. *9*, e1003432.

Katlama, C., Deeks, S.G., Autran, B., Martinez-Picado, J., van Lunzen, J., Rouzioux, C., Miller, M., Vella, S., Schmitz, J.E., Ahlers, J., et al. (2013). Barriers to a cure for HIV: new ways to target and eradicate HIV-1 reservoirs. Lancet *381*, 2109–2117.

Khoury, G., Anderson, J.L., Fromentin, R., Hartogenesis, W., Smith, M.Z., Bacchetti, P., Hecht, F.M., Chomont, N., Cameron, P.U., Deeks, S.G., and Lewin, S.R. (2016). Persistence of integrated HIV DNA in CXCR3 + CCR6 + memory CD4+ T cells in HIV-infected individuals on antiretroviral therapy. AIDS *30*, 1511.

Kwon, K.J., Timmons, A.E., Sengupta, S., Simonetti, F.S., Zhang, H., Hoh, R., Deeks, S.G., Siliciano, J.D., Siliciano, R.F., et al. (2020). Different human resting memory CD4+ T cell subsets show similar low inducibility of latent HIV-1 proviruses. Sci. Transl. Med. *12*, eaax6795.

Laanani, M., Ghosn, J., Essat, A., Melard, A., Seng, R., Gousset, M., Panjo, H., Mortier, E., Girard, P.M., Goujard, C., et al. (2015). Impact of the timing of initiation of antiretroviral therapy during primary HIV-1 infection on the decay of cell-associated HIV-DNA. Clin. Infect. Dis. *60*, 1715.

Laird, G.M., Eisele, E.E., Rabi, S.A., Lai, J., Chioma, S., Blankson, J.N., Siliciano, J.D., and Siliciano, R.F. (2013). Rapid quantification of the latent reservoir for HIV-1 using a viral outgrowth assay. Plos Pathog. *9*, e1003398.

Lee, E., Bacchetti, P., Milush, J., Shao, W., Boritz, E., Douek, D., Fromentin, R., Liegler, T., Hoh, R., Steve, G., et al. (2019). Memory CD4 + T-cells expressing HLA-DR contribute to HIV persistence during prolonged antiretroviral therapy. Front. Microbiol. *10*, 2214.

Van Lint, C., Bouchat, S., and Marcello, A. (2013). HIV-1 transcription and latency: an update. Retrovirology *10*, 67.

Llewellyn, G.N., Seclén, E., Wietgrefe, S., Liu, S., Chateau, M., Pei, H., Perkey, K., Marsden, M.D., Hinkley, S.J., Paschon, D.E., et al. (2019). Humanized mouse model of HIV-1 latency with enrichment of latent virus in PD-1 + and TIGIT + CD4 T cells. J. Virol., e02086-18.

Lorenzo-Redondo, R., Fryer, H.R., Bedford, T., Kim, E.Y., Archer, J., Pond, S.L.K., Chung, Y.S., Penugonda, S., Chipman, J., Fletcher, C.V., et al. (2016). Persistent HIV-1 replication maintains the tissue reservoir during therapy. Nature *530*, 51.

Lundgren, J.D., Lundgren, J.D., Babiker, A.G., Gordin, F., Emery, S., Grund, B., Sharma, S., Avihingsanon, A., Cooper, D.A., Fätkenheuer, G., et al. (2015). Initiation of antiretroviral therapy in early asymptomatic HIV infection. N. Engl. J. Med. *373*, 795–807.

Marsden, M.D., Loy, B.A., Wu, X., Ramirez, C.M., Schrier, A.J., Murray, D., Shimizu, A., Ryckbosch, S.M., Near, K.E., Chun, T.W., et al. (2017). In vivo activation of latent HIV with a synthetic bryostatin analog effects both latent cell "kick" and "kill" in strategy for virus eradication. Plos Pathog. *13*, e1006575.

Marsden, M.D., and Zack, J.A. (2017). Humanized mouse models for human immunodeficiency virus infection. Annu. Rev. Virol. *4*, 393–412.

Martin, G.E., Pace, M., Thornhill, J.P., Phetsouphanh, C., Meyerowitz, J., Gossez, M., Brown, H., Olejniczak, N., Lwanga, J., Ramjee, G., et al. (2018). CD32-expressing CD4 T cells are phenotypically diverse and can contain proviral HIV DNA. Front. Immunol. *9*, 928.

Martinez-Picado, J., and Deeks, S.G. (2016). Persistent HIV-1 replication during antiretroviral therapy. Curr. Opin. HIV AIDS *11*, 417.

Murray, A.J., Kwon, K.J., Farber, D.L., and Siliciano, R.F. (2016). The latent reservoir for HIV-1: how immunologic memory and clonal expansion contribute to HIV-1 persistence. J. Immunol. *197*, 407.

Namazi, G., Fajnzylber, J.M., Aga, E., Bosch, R.J., Acosta, E.P., Sharaf, R., Hartogensis, W., Jacobson, J.M., Connick, E., Volberding, P., et al. (2018). The control of HIV after antiretroviral medication pause (CHAMP) study: posttreatment controllers identified from 14 clinical studies. J. Infect. Dis. *218*, 1954–1963.

Nischang, M., Sutmuller, R., Gers-Huber, G., Audigé, A., Li, D., Rochat, M.A., Baenziger, S., Hofer, U., Schlaepfer, E., Regenass, S., et al. (2012). Humanized mice recapitulate key features of HIV-1 infection: a novel concept using long-acting anti-retroviral drugs for treating HIV-1. PLoS One *7*, e38853.

Noto, A., Procopio, F.A., Banga, R., Suffiotti, M., Corpataux, J.M., Cavassini, M., Riva, A., Fenwick, C., Gottardo, R., Perreau, M., and Pantaleo, G. (2018). CD32. J. Virol. *92*.

Osuna, C.E., Lim, S.-Y., Kublin, J.L., Apps, R., Chen, E., Mota, T.M., Huang, S.-H., Ren, Y., Bachtel, N.D., Tsibris, A.M., et al. (2018). Evidence that CD32a does not mark the HIV-1 latent reservoir. Nature *561*, E20–E28.

Palmer, S., Josefsson, L., and Coffin, J.M. (2011). HIV reservoirs and the possibility of a cure for HIV infection. J. Intern. Med. *270*, 550–560.

Panel on Antiretroviral Guidelines for Adults and Adolescents (2017). Guidelines for the Use of Antiretroviral Agents in Adults and Adolescents Living with HIV (Department of Health and Human Services).

Pérez, L., Anderson, J., Chipman, J., Thorkelson, A., Chun, T.K., Moir, S., Haase, A.T., Douek, D.C., Timothy, W., Schacker, T.W., et al. (2018). Conflicting evidence for HIV enrichment in CD32+ CD4 T cells. Nature *561*, E9–E16.

Policicchio, B.B., Pandrea, I., and Apetrei, C. (2016). Animal models for HIV cure research. Front. Immunol. *7*, 12.

Rothenberger, M., Nganou-Makamdop, K., Kityo, C., Ssali, F., Chipman, J.G., Beilman, G.J., Hoskuldsson, T., Anderson, J., Jasurda, J., Schmidt, T.E., et al. (2019). Impact of integrase inhibition compared with nonnucleoside inhibition on HIV reservoirs in lymphoid tissues. J. Acquir. Immune Defic. Syndr. *81*, 355–360.

Sáez-Cirión, A., Bacchus, C., Hocqueloux, L., Avettand-Fenoel, V., Girault, I., Lecuroux, C., Potard, V., Versmisse, P., Melard, A., Prazuck, T., et al. (2013). Post-Treatment HIV-1 controllers with a long-term virological remission after the interruption of early initiated antiretroviral therapy ANRS VISCONTI study. Plos Pathog. *9*, e1003211.

Satheesan, S., Li, H., Burnett, J.C., Takahashi, M., Li, S., Wu, S.X., Synold, T.W., Rossi, J.J., and Zhou, J. (2018). HIV replication and latency in a humanized NSG mouse model during suppressive oral combinational antiretroviral therapy. J. Virol. *92*, e02118–17.

De Scheerder, M.A., Vrancken, B., Dellicour, S., Schlub, T., Lee, E., Shao, W., Rutsaert, S., Verhofstede, C., Kerre, T., Malfait, T., et al. (2019). HIV rebound is predominantly fueled by genetically identical viral expansions from diverse reservoirs. Cell Host Microb *26*, 347–358.e7.

Siliciano, J.D., Kajdas, J., Finzi, D., Quinn, T.Q., Chadwick, K., Margolick, J.B., Kovacs, C., Gange, S.J., and Siliciano, R.F. (2003). Long-term follow-up studies confirm the stability of the latent reservoir for HIV-1 in resting CD4+ T cells. Nat. Med. *9*, 727–728.

Siliciano, J.D., et al. (2003b). Long-term follow-up studies confirm the stability of the latent reservoir for HIV-1 in resting CD4+ T cells. Nat. Med. *9*, 727–728.

Soriano-Sarabia, N., Bateson, R.E., Dahl, N.P., Crooks, A.M., Kuruc, J.D., Margolis, D.M., and Archin, N.M. (2014). Quantitation of replication-competent HIV-1 in populations of resting CD4+ T cells. J. Virol. *88*, 14070–14077.

Ssebunya, R., Wanyenze, R.K., Lukolyo, H., Mutto, M., Kisitu, G., Amuge, P., Maganda, A., and Kekitiinwa, A. (2017). Antiretroviral therapy initiation within seven days of enrolment: outcomes and time to undetectable viral load among children at an urban HIV clinic in Uganda. BMC Infect. Dis. *17*, 439.

Strain, M.C., Little, S.J., Daar, E.S., Havlir, D.V., Gunthard, H.F., Lam, R.Y., Daly, O.A., Nguyen, J., Ignacio, C.C., Spina, C.A., et al. (2005). Effect of treatment, during primary infection, on establishment and clearance of cellular reservoirs of HIV-1. J. Infect. Dis. *191*, 1410–1418.

Thornhill, J.P., Pace, M., Martin, G.E., Hoare, J., Peake, S., Herrera, C., Phetsouphanh, C., Meyerowitz, J., Hopkins, E., Brown, H., et al. (2019). CD32 expressing doublets in HIV-infected gut-associated lymphoid tissue are associated with a T follicular helper cell phenotype. Mucosal Immunol. *12*, 1212–1219.

Trautmann, L., Janbazian, L., Chomont, N., Said, E.A., Gimmig, S., Bessette, B., Boulassel, M.-R., Delwart, E., Sepulveda, H., Balderas, R.S., et al. (2006). Upregulation of PD-1 expression on HIV-specific CD8+ T cells leads to reversible immune dysfunction. Nat. Med. *12*, 1198–1202.

Vasquez, J.J., Aguilar-Rodriguez, B.L., Rodriguez, L., Hogan, L.E., Somsouk, M., McCune, J.M., Deeks, S.G., Laszik, Z.G., Hunt, P.W., and Henrich, T.J. (2019). CD32-RNA Co-localizes with HIV-RNA in CD3+ cells found within gut tissues from viremic and ART-suppressed individuals. Pathog. Immun. *3*, 147–160.

Whitney, J.B., Hill, A.L., Sanisetty, S., Penaloza-MacMaster, P., Liu, J., Shetty, M., Parenteau, L., Cabral, C., Shields, J., Blackmore, S., et al. (2014). Rapid seeding of the viral reservoir prior to SIV viraemia in rhesus monkeys. Nature *512*, 74–77.

Whitney, J.B., and Brad Jones, R. (2018). In vitro and in vivo models of HIV latency. Adv. Exp. Med. Biol. 241–263.

Williams, J.P., Hurst, J., Stöhr, W., Robinson, N., Brown, H., Fisher, M., Kinloch, S., Cooper, D., Schechter, M., Tambussi, G., et al. (2014). HIV-1 DNA predicts disease progression and post-treatment virological control. Elife *12*, e03821.

Wittner, M., Dunay, G.A., Kummer, S., Bockhorn, M., Hüfner, A., Schmiedel, S., Degen, O., van Lunzen, J., Eberhard, J.M., and Schulze Zur Wiesch, J. (2018). CD32 expression of different memory t cell subpopulations in the blood and lymph nodal tissue of HIV patients and healthy controls correlates with immune activation. J. Acquir. Immune Def. Syndr. *77*, 345–349.

Zerbato, J.M., McMahon, D.K., Sobolewski, M.D., Mellors, J.W., Sluis-Cremer, N., et al. (2019). Naive CD4+ T cells harbor a large inducible reservoir of latent, replication-competent human immunodeficiency virus type 1. Clin. Infect. Dis. *69*, 1919–1925.

iScience, Volume *24*

Supplemental Information

$CD32^{+}CD4^{+}$ memory T cells are enriched for total HIV-1 DNA in tissues from humanized mice

Philipp Adams, Virginie Fievez, Rafaëla Schober, Mathieu Amand, Gilles Iserentant, Sofie Rutsaert, Géraldine Dessilly, Guido Vanham, Fanny Hedin, Antonio Cosma, Michel Moutschen, Linos Vandekerckhove, and Carole Seguin-Devaux

SUPPLEMENTAL INFORMATION

Transparent methods section

NSG mice immune reconstitution, HIV-1 infection and treatment with cART

NSG (NOD/LtSz-scid/IL2Rγnull) mice were purchased from Jackson Laboratory, USA. All animal experiments were performed in accordance with the Animal Welfare Structure of the Luxemburg Institute of Health (LIH) (protocol number: LRTV 1402) and complied with the national legislation and guidelines for animal experimentation. Juvenile (3-4 weeks of age) NSG mice were engrafted as previously published (Singh *et al.*, 2012). Briefly, mice were conditioned by two intraperitoneal Busulfan injections (20 mg/kg, Busilvex®) 24 and 12 hours before transplantation. CD34+ hematopoietic stem cells were isolated from human cord blood, provided by the Blood Bank of the University Hospital (Liège, Belgium), by magnetic activated cell sorting (MACS), using the CD34+ progenitor cell isolation kit (Stem Cell Technologies, Vancouver, Canada). Subsequently $2x10^5$ freshly isolated CD34+ cells were transplanted into each NSG mouse by intravenous injection. Mice were bled at 12 and 24 weeks post-transplantation to determine human immune cell reconstitution by flow cytometry.

Animals with ≥ 20% of circulating human $CD45^+$ cells at 24 weeks post-transplantation were infected by two intraperitoneal injections of a HIV-1 laboratory adapted strain (JRCSF, 10.000 TCID50) within 24 hours. Infection was monitored every 2 weeks on blood samples collected by submandibular bleeding for $CD4^+$ T cell counting using flow cytometry analysis and for viral load measurement (see below). cART treatment was initiated 1 week (early treated) or 8 weeks (late treated) post infection and continued for a total of 8 weeks in both groups using a single tablet regimen of dolutegravir/abacavir/lamivudine (Triumeq®, ViiV Healthcare) provided in the drinking water. The tablets were crushed and dissolved in Sucralose MediDrop® (Clear H_2O, Portland, USA) at the therapeutic concentration of 3.40 mg/ml. Drinking solution was refreshed twice per week and volumes were monitored to follow up consumption. At the end of the protocol, mice were anesthetized using a mixture of ketamine and xylazine, blood samples were collected via cardiac puncture and tissues were harvested for downstream analysis.

Experimental design

The study was structured into three arms (Figure 1). A first group of mice infected with HIV-1 received treatment from one week post infection on (early treated, n= 58). The second group was set on therapy at week seven post-infection (late treated, n=42) and a third group of HIV-1 infected mice never received

antiretroviral drugs (untreated, n=20). After eight weeks of cART treatment, animals were sacrificed (n= 43 and 34 in early and late treated groups). Some animals was kept after cART was discontinued to measure time to viral detectability after treatment interuption. These groups of "viral rebound" were monitored for another six weeks (n=15 for early- and n=8 for late treated mice) or longer if they remained undetectable in plasma viral loads. Untreated animals were sacrificed at the matched time points with the early and late treated mice respectively (n=10 for each group). Non-infected and non-treated humanized mice (healthy animals) were added as controls when necessary for phenotyping. Monitoring of viral load upon HIV-1 infection and under cART treatment was performed using absolute ddPCR measurement every two weeks.

Organ collection, processing and isolation of cells

Organs were collected at necropsy, washed in cold RPMI and processed immediately for cell isolation. Lymph nodes were dissected from the cervical, axillary, brachial and inguinal locations. Spleens and lymph nodes were gently disrupted in cold PBS using the plunger of a syringe. Bone marrow (BM) were obtained from tibias and femurs. Both ends of bones were opened and BM flushed out by short centrifugation at 600g during 30 seconds at room temperature. BM cells, splenocytes and lymph node suspensions were passed through 70 µm nylon cell strainers (BD Biosciences, Franklin-Lakes, New Jersey, USA) and centrifuged 10 min at 400g and 4°C. Splenocytes were resuspended in fresh ACK (Ammonium-Chloride-Potassium) solution (in house made) for 5 minutes to lyse red blood cell followed by two washes with RPMI 1640 (GIBCO Life technologies, Thermo Fisher Scientific).

Quantification of HIV-1 plasma and tissues viral load

Plasma viral load was measured by an in-house droplet digital PCR (ddPCR) assay. Input volumes of 100 µl were used for RNA extraction using the MagNA Pure Compact nucleic acid isolation kit (Roche, Basel, Switzerland) according to the manufacturer's protocol by diluting 30 µl of mice plasma in 70 µl of PBS. The PCR reaction mixture was loaded into the Bio-Rad QX200™ Droplet Generator (Bio-Rad laboratories, Hercules, CA, USA)**.** Emulsification droplets were formed following the manufacturer's instructions. Primers and probes were designed as reported previously (Jones *et al.*, 2014). Total RNA was amplified by ddPCR PalmerddPCR Advanced kit for Probes. Droplets were analyzed on QX200 Droplet Reader (BioRad). The limit of detection is 235 copies/ml (33). Data were analyzed with the QuantaSoft software (Bio-Rad laboratories, Hercules, CA, USA). To measure HIV-1 RNA in different tissues, twelve humanized mice (as described above) were infected by two intraperitoneal injections of HIV-1 (JRCSF, 10.000 TCID50) within 24 hours. One week after infection, six mice were sacrificed for downstream analysis and six mice started cART as previously described and continued for a total of eight weeks. Plasma viral load was monitored every 2 weeks on blood samples collected by submandibular bleeding. At the end of cART treatment, mice were sacrificed for organ

collection and all organs were processed immediately for cell isolation using the NucleoSpin® Tissue kit (Macherey-Nagel, Düren, Germany). 300uL lysis buffer was used for RNA extraction in the spleen and the bone marrow and 100uL of lysis buffer was used for the Lymph nodes. Input volumes of 100 µl were used for plasma RNA extraction using the QIAamp Vrial RNA Mini Kit (Qiagen) according to the manufacturer's protocol. Plasma and organ viral loads were measured by our in-house droplet digital PCR (ddPCR) assay as described above.

Quantification of total Cell-associated (CA)-HIV-1 DNA and CA-HIV-1 RNA from human CD45$^+$ cells

Human CD45$^+$ cells from organs were purified by positive selection using magnetic beads (CD45 MicroBeads, Miltenyi Biotec, Bergisch-Gladbach, Germany) following the instructions of the manufacturer and pelleted. Total DNA was extracted from spleen, lymph nodes, lungs and bone marrow cells by manual extraction using the NucleoSpin® Tissue kit (Macherey-Nagel, Düren, Germany) according to manufacturer's instructions. Aliquots of eluted samples were frozen at −80 °C until total CA HIV-1 DNA quantification by ddPCR as previously reported (Rutsaert *et al.*, 2019). RNA was isolated from human CD45$^+$ cells using the innuPrep RNA Mini Kit 2.0 (Westburg, Berlin, Germany), then reverse transcribed into cDNA using qScript cDNA SuperMix (Quanta bio, Beverly, Massachusetts, USA) in a total volume of 20µl according to manufacturer's protocol. CA HIV-1 RNA was measured by ddPCR (Bio-Rad, Hercules, California) in triplicates as previously described (Van Hecke *et al.*, 2019) with the primers/probe as described above for HIV-1 DNA. Three reference genes (B2M, ACTB, and GAPDH) per cDNA samples were assessed by qPCR to normalize for RNA input. Copies of CA-RNA were divided by the geometric mean of the reference gene related to the theoretical number of cells (expressed in copies per million cells).

Flow cytometry, cell sorting and image cytometry

Detailed phenotyping of human B and T cells was performed using 2x10^6 single cells from each organ. Cells were washed with PBS containing 1%FBS (Gibco™, Thermo Fisher Scientific, Waltham, Massachusetts, USA) and stained for 30 min at 4°C with fluorochrome-labeled monoclonal antibodies (human reactivity if not indicated differently): CD4-BUV395 (SK3), CD3-BUV496 (UCHT1), CD8-BUV805 (SK1), CD279-BV421 (EH12.2H7), CD28-BV605(CD28.2), CD27-BV650(M-T271), CD197-PECF-594 (150305), murineCD45RO-PECy5 (30-F11) from BD Biosciences, HLA-DR-BV510 (L243), CD127-BV711(HIL-7R-M21), CD32-PE (FUN-2), TIGIT-APC (A151536) from Biolegend (San Diego, CA, USA) and LIVE/DEAD fixable Near-IR cell dye (Thermo Fisher Scientific). Cells were fixed for 1h at 4°C using 1X BD Lysing solution (BD Biosciences, Cat n°: 349202) before acquisition. Samples were acquired on a FACS Fortessa SORP 5 laser instrument (BD Biosciences) and

analyzed with the Kaluza (version 2.1, Beckman Coulter, Brea, California, USA) and Flow Jo (version 10, BD Biosciences) softwares. A Two-way cell sorting was done by staining single cells derived from organs with CD3-BV510 (UCHT-1), CD4-PECy7 (RPA-T4), CD8-BV711 (RPA-T8), CD19-APC (HIB19), CD14-APC (61D3), CD45RA-FITC (HI100), murineCD45-PECy5 (30-F11) (BD Biosciences) and CD32-PE (FUN-2) (Biolegend), and LIVE/DEAD fixable Near-IR cell dye (Thermo Fisher Scientific). $CD4^+CD45RA^-$ memory T cells were sorted based on their expression of CD32 into positive and negative subsets using BD Influx instrument (BD Biosciences). For visualization of sorted cells ($CD32^+CD4^+$ T cells and B cells) sorting was executed with five laser ARIA cell sorter (BD Biosciences) and purified populations were acquired with the ImagestreamX (Amnis Corporation, Seattle, WA, USA). mCD45-FITC (30-F11), CD4-PE-CF594 (RPA-T4), CD20-BV421 (2H7), CD3-BV510 (UCHT1), CD32-APC (FLI8.26) (BD Biosciences), CD19-PE (SJ25C1) (Biolegend), CD14-PECy5 (61D3) (eBiosciences) and LIVE/DEAD fixable Near-IR cell dye (Thermo Fisher Scientific).The detailed gating strategy for all cytometry application on CD4+ T cells for strict exclusion of CD19, CD14 and doublets is given in supplemental Figure 3. PBMCs from two HIV-1 infected patients under cART for more than 2 years were also analyzed as previously described. The study was approved by the Ethical Committee of Luxembourg (201307/10). The two patients provided their written informed consent to participate in the study.

Measurement of CD32a and CD32b mRNA

To determine the CD32 isoform expressed in the memory $CD4^+$ T cells, BM cells and splenocytes from 3 mice infected with HIV-1 and treated early with cART during 8 weeks were isolated as described above. Nucleic acids were extracted from sorted $CD32^+CD45RA^-CD4^+$ T cells, $CD32^-CD45RA^-$ $CD4^+$ T cells and a pool of $CD14^+$ and $CD19^+$ cells from the spleen and the bone marrow using Nucleospin RNA XS (Marcherey Nagel, Germany) and treated with DNase (DNA-free kit, Thermo Fisher Scientific) following manufactor's instructions. For the $CD32^+CD45RA^-$ $CD4^+$ T cell fraction, cells from the 3 spleens or from the 3 BM were pooled before RNA extraction whereas the nucleic acids from the two other fractions of cells ($CD45RA^-$ $CD4^+CD32^-$ T cells and a pool of $CD14^+$ and $CD19^+$ cells) were extracted for each mouse individually. Reverse transcription was executed using the High-Capacity RNA-to-cDNA™ Kit (Thermo Fisher Scientific) according to manufacturer's instructions. Cellular mRNAs were quantified using TaqMan™ Gene Expression Assays (all from Thermo Fisher Scientific): CD32A: Hs01013401_g1, CD32B: Hs00269610_m1, GAPDH: Hs02758991_g1 using Real-Time PCR (ABI 7500 Fast, Thermo Fisher Scientific). Non-template control wells were included in every qPCR run and were consistently negative.

Cluster analysis and multidimensional reduction

To investigate the relationship between CD32 expression and the activation status of $CD4^+$ and $CD8^+$ T cells, three groups were without treatment (n=8), early treatment (n=12) and late treatment (n=10). The three groups of mice were phenotyped at four weeks and eight weeks of HIV-1 infection or four and eight weeks of treatment. Splenocytes were harvested and flow cytometry was performed as described above. Between 207 and 793506 live $CD3^+CD14^-CD19^-$ T cells were gated for each sample using FlowJo (BD Bioscience, version 10.7). Live $CD3^+CD14^-CD19^-$ T cells were exported as FCS files and uploaded into the Cytobank environment (Beckman Coulter). After proper scaling for each marker (Mazza *et al.*, 2018) the FlowSOM algorithm (Van Gassen *et al.*, 2015) was used to generate 49 clusters grouped in ten metaclusters. FlowSOM parameters were as follow: 4 millions of proportionally selected events; clustering channels: CD4, CD8, CD145RA, CCR7, TIGIT, PD1, HLADR, CD32 and CD38; iteration number: 10. Hierarchical analysis, heatmap and statistical analyses (Kruskal Wallis tests) were done in Qlucore version 3.6 (Lund, Sweden).

Quantification of translation-competent viral reservoirs

The HIV-1 Flow assay was used as previously described (Pardons *et al.*, 2019) to quantify the amount of the p24 producing HIV-1 reservoir in human $CD4^+$ $CD32^+$ versus $CD4^+$ $CD32^-$ T cells. Briefly, cells were harvested from spleen and bone marrow of HIV-1 infected cART suppressed mice (late protocol, as described above) and cultured in RPMI (10% Fetal Bovine Serum and 2% Penstrep) supplemented with antiretroviral drugs (200nM raltegravir, 200nM lamivudine). A protein transport inhibitor (Golgi Plug, BD Biosciences) was added according to manufacturer's instruction 1 hour before stimulation and maintained during stimulation with PMA (162nM/mL) and Ionomycin (1µg/mL) for 24 hours. Cells were stained for surface markers and the intracellular p24 protein (anti-p24 PE, clone: KC57, Beckmann Coulter and anti-p24 APC, clone: 28B7, MediMabs, Canada) using the BD Cytofix/Cytoperm staining kit (BD Biosciences). Extracellular expression of CD32 combined with activation/exhaustion markers and the intracellular staining of p24 was performed as described above.

Statistical analysis

Statistical analysis was performed using GRAPHPAD PRISM software. Groups were compared using nonparametric Mann-Whitney *U* test or Kruskal Wallis with Dunn correction for multiple comparison. A p-values < 0.05 was considered to be significant. Two-tailed Spearman correlation coefficient was calculated for several comparisons (r and p values indicated on respective graphs). Mantel-Cox rank test was applied for Kaplan Meyer curve comparison. Paired or unpaired Wilcoxon signed-rank test were used when indicated. For all statistical testings a p-values < 0.05 was considered to name as significant in the text. The following

symbols were used as abbreviations for results of statistical significance testing on figures, p values: * ≤ 0.05, **≤ 0.005, *** ≤ 0.0005, **** ≤ 0.00005, Abbreviation ns stands for non-significant.

Supplemental references

Singh, M. *et al.* (2012) 'An improved protocol for efficient engraftment in NOD/LTSZ-SCIDIL-2RγNULL mice allows HIV replication and development of anti-HIV immune responses', *PLoS ONE*, 7(6).
Jones, M. *et al.* (2014) 'Low copy target detection by Droplet Digital PCR through application of a novel open access bioinformatic pipeline, "definetherain"', *Journal of Virological Methods*, 202, 46–53.
Rutsaert, S. *et al.* (2019) 'Evaluation of HIV-1 reservoir levels as possible markers for virological failure during boosted darunavir monotherapy', *The Journal of antimicrobial chemotherapy*.
Van Hecke, C. *et al.* (2019) 'Early treated HIV-1 positive individuals demonstrate similar restriction factor expression profile as long-term non-progressors', *EBioMedicine*.
Mazza, E. M. C. *et al.* (2018) 'Background fluorescence and spreading error are major contributors of variability in high-dimensional flow cytometry data visualization by t-distributed stochastic neighboring embedding', *Cytometry Part A*.
Van Gassen, S. *et al.* (2015) 'FlowSOM: Using self-organizing maps for visualization and interpretation of cytometry data', *Cytometry Part A*.
Pardons, M. *et al.* (2019) 'Single-cell characterization and quantification of translation-competent viral reservoirs in treated and untreated HIV infection', *PLoS Pathogens*.

Supplemental figures

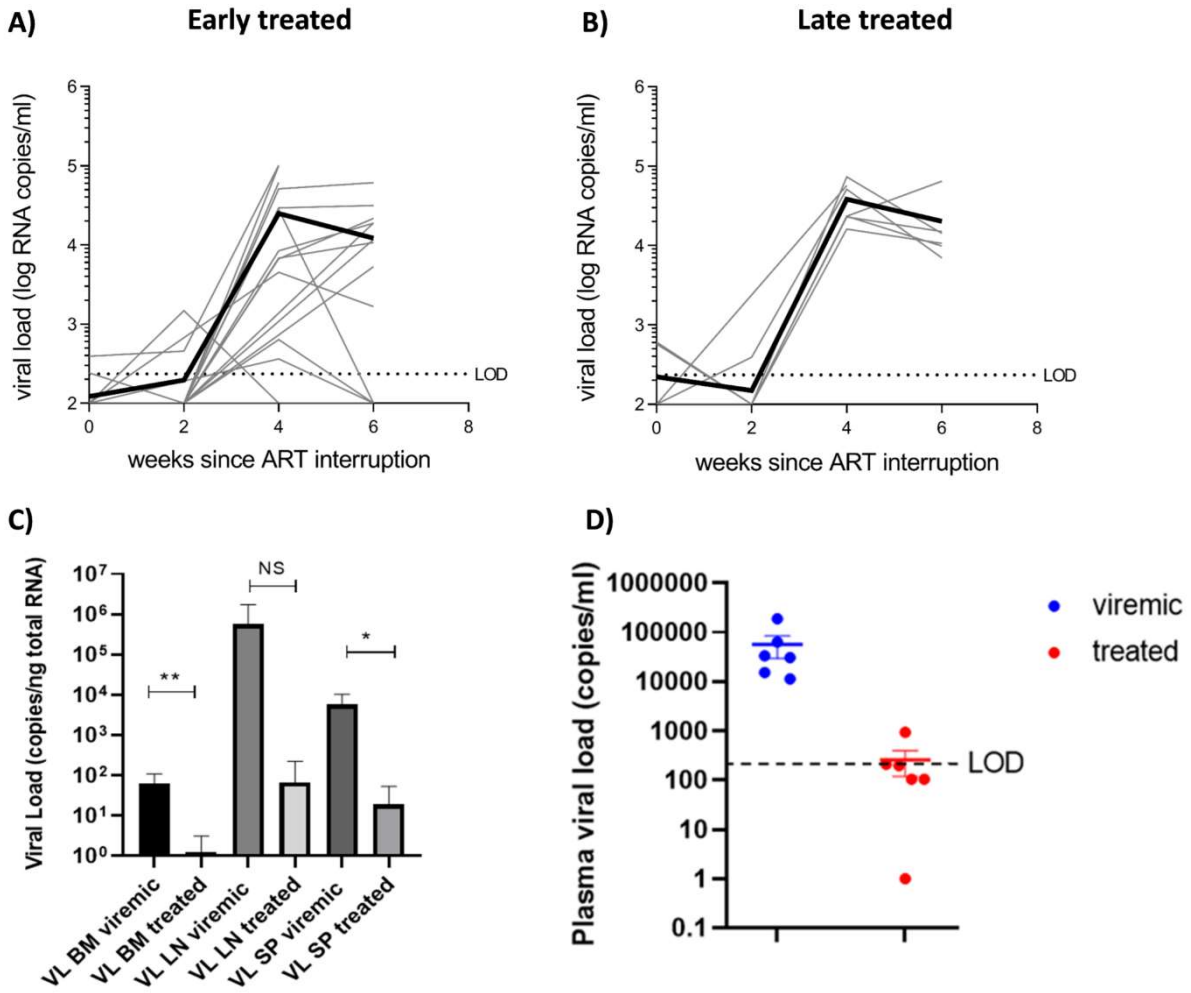

Figure S1 related to Figure1. Viral rebound after cART interruption in early versus late treated mice and HIV RNA content in tissues from viremic and virally suppressed mice.

Individual values of HIV-1 RNA copies in log10 scale per ml of blood plasma over time after treatment interruption in light grey lines in mice treated early after 1 week of HIV-1 infection (A) and in mice treated late (B) (Group mean in bold black line). Four mice treated early reached undetectable viral load four or six weeks after treatment interruption. C. HIV-1 RNA content in different tissues of viremic and virally suppressed humanized mice. Twelve mice were infected with HIV-1 by two intraperitoneal injections of HIV-1 JRCSF (10.000 TCID50) within 24 hours. Six mice were sacrificed one week after infection (viremic mice) and six mice were treated with cART during 8 weeks after one week of infection and sacrificed to measure viral load (VL, HIV-1 RNA) in the bone marrow (BM), in the lymph nodes (LN) and in the spleen (SP). One mouse did not reach HIV-1 RNA undetectability after 8 weeks of treatment. In the BM, HIV-1 RNA is not detectable after 8 weeks of cART whereas a mean of 100 copies/ng of total RNA was measured in the lymph nodes and in the spleen of the early treated mice. D). Plasma viral load of the viremic and virally suppressed humanized mice. Statistical testing was done using non-parametric Kruskal Wallis test with multiple comparison Dunn's correction (* $p< 0.05$. ** $p< 0.01$, NS, non significant test, $p> 0.05$).

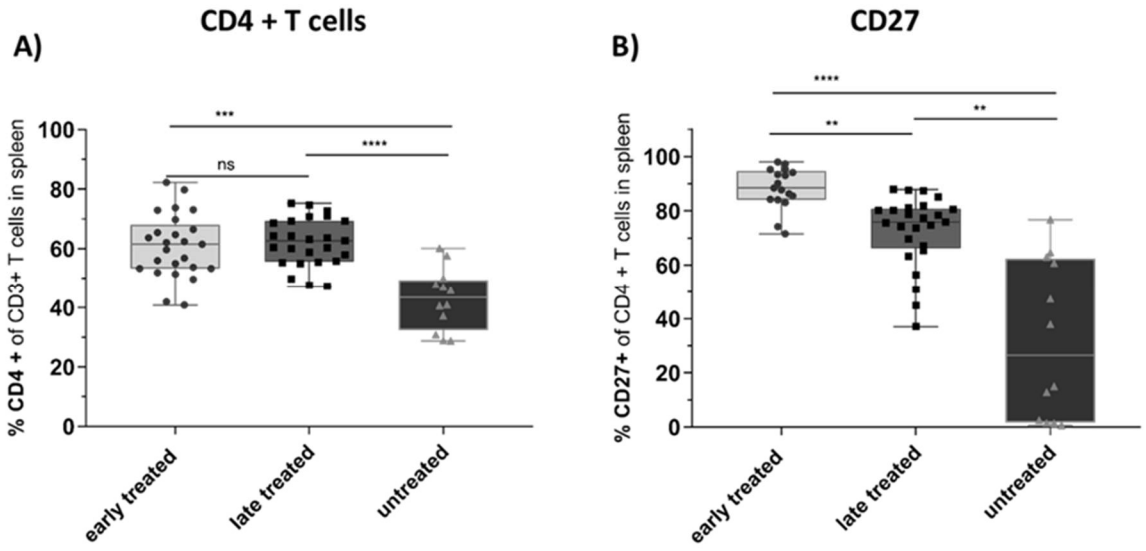

Figure S2 related to Figure 2. CD4$^+$ T cells were preserved by ART in the spleen of humanized mice.
Relative percentage of CD4$^+$ T cells (A) and CD27 expression in CD4$^+$ T cells (B). Statistical testing was done using non-parametric Kruskal Wallis test with multiple comparison Dunn's correction (**p< 0.01, *** p< 0.005, **** p < 0.001, ns, non significant test, p> 0.05).

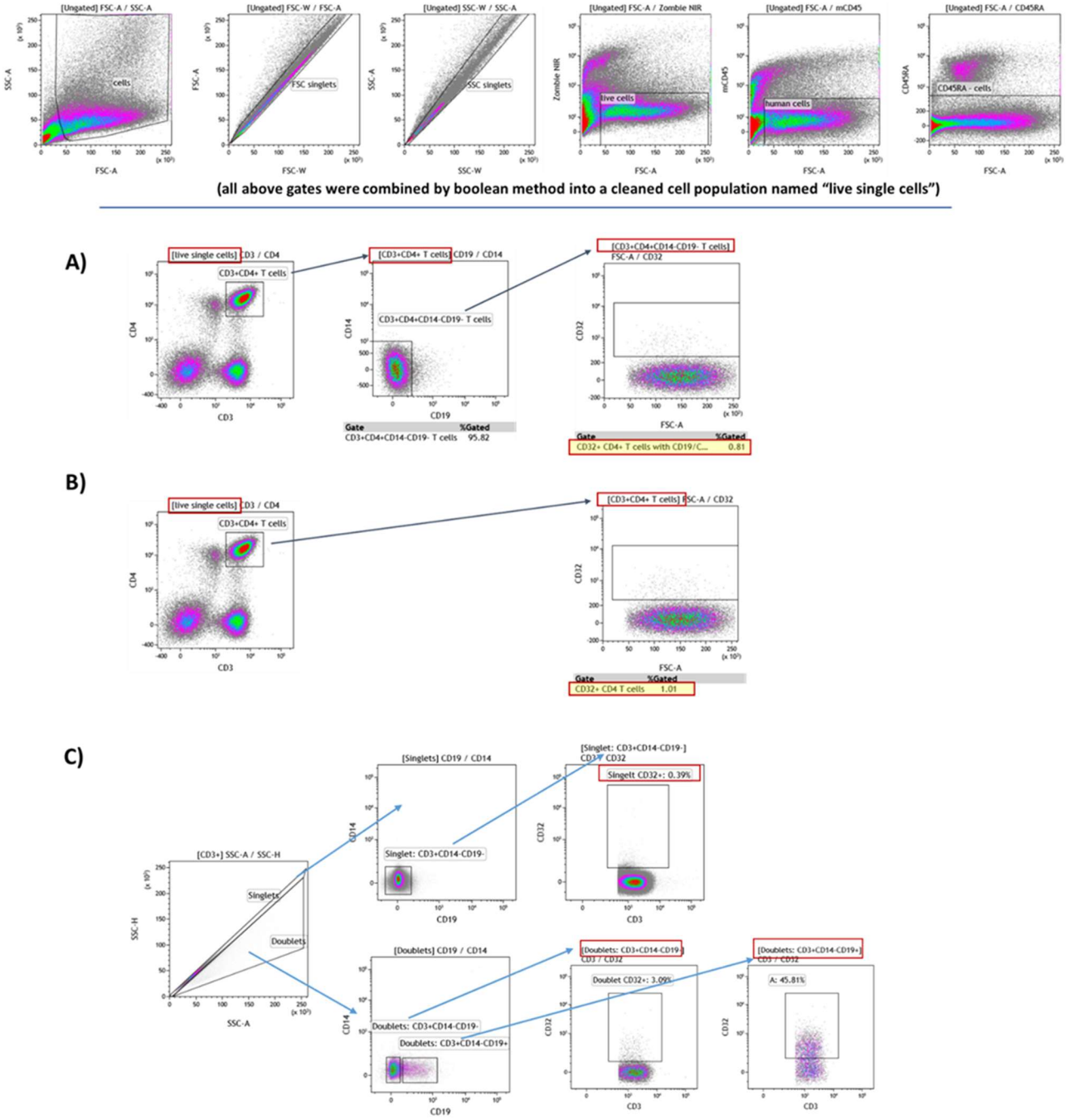

Figure S3 Related to Figures 4 and Figures 5. Flow cytometry gating strategy for the phenotypic investigation of CD32^{+}CD4^{+} T cells.

Following a lineage gating strategy (top layer) we strictly gated on singlet cells and further excluded potential contaminations by gating on negative events for CD14 and CD19, leading to a highly pure CD32 ^{dim} T cell population. In contrast clear doublet cells of T and B cells are detected leading to a CD32 ^{Bright} population in the doublets CD3^{+}CD14^{-}CD19^{-} and CD3^{+}CD14^{-}CD19^{+}cells.

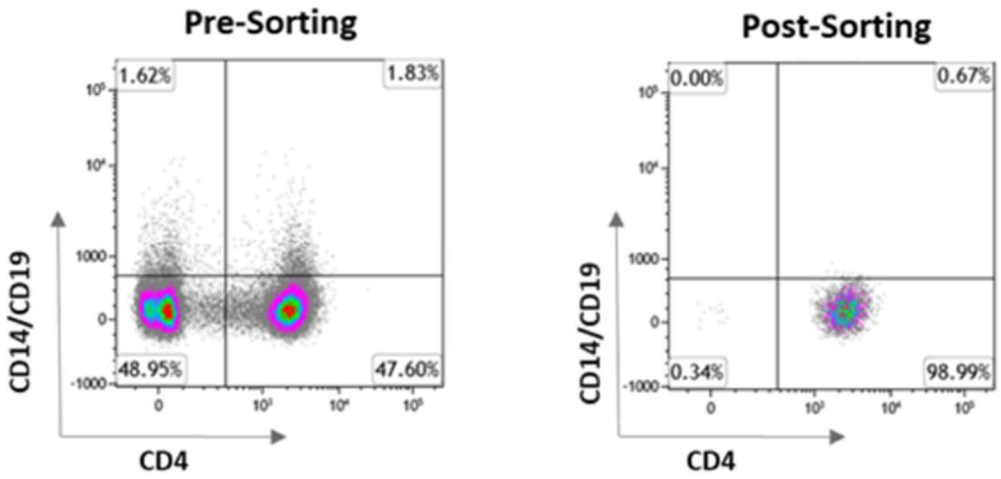

Figure S4 Related to Figures 4 and 5. Purity of CD4+CD32+ T cells before and after sorting from splenocytes of humanized mice using the established gating strategy (Figure S3).

Representative plots depicting the expression of CD14/CD19 and CD4 in CD4+CD32+ T cells sorted from splenocytes of humanized mice. Cells were gated on lymphocytes (singlets and live cells) before (Pre-Sorting) and after (Post-Sorting) cell sorting of CD4+CD32+ T cells. The purity was assessed on four different mice revealing a mean purity of 98,85%.

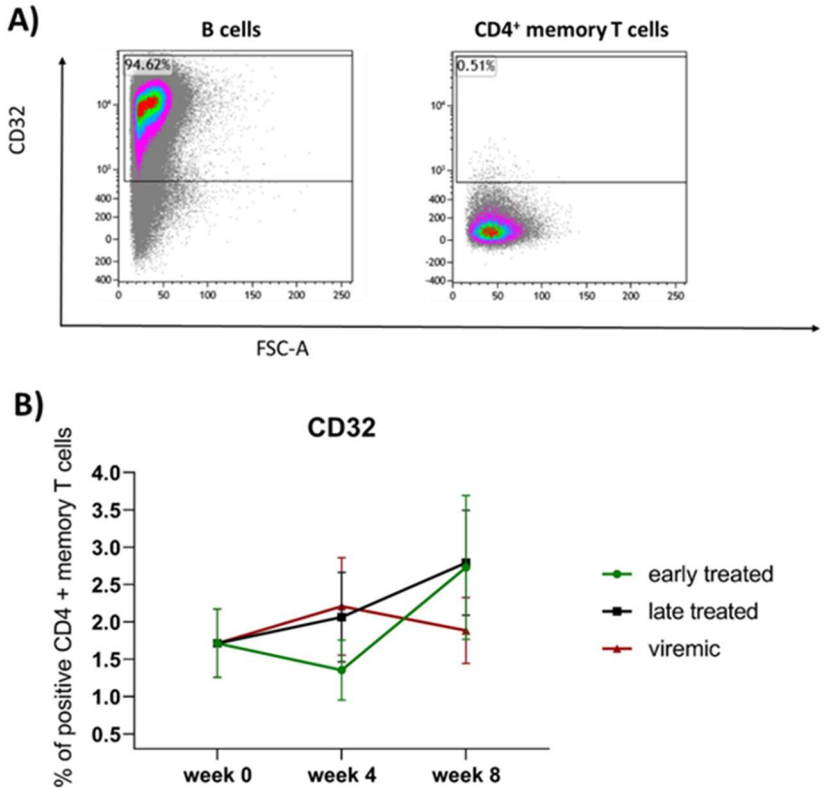

Figure S5 related to Figure 5. Longitudinal expression of CD32 in CD4⁺ memory T cells from spleen
Representative FACS plots of CD32 expression on B cells and CD4⁺ memory T cells (A). CD32 expression on CD4⁺ memory T cells from spleen did not differ significantly over time between treatment groups (B). Three groups of mice were infected with HIV-1: viremic, untreated mice (n= 12), mice receiving early cART treatment (n= 12) or late treatment (n= 10).

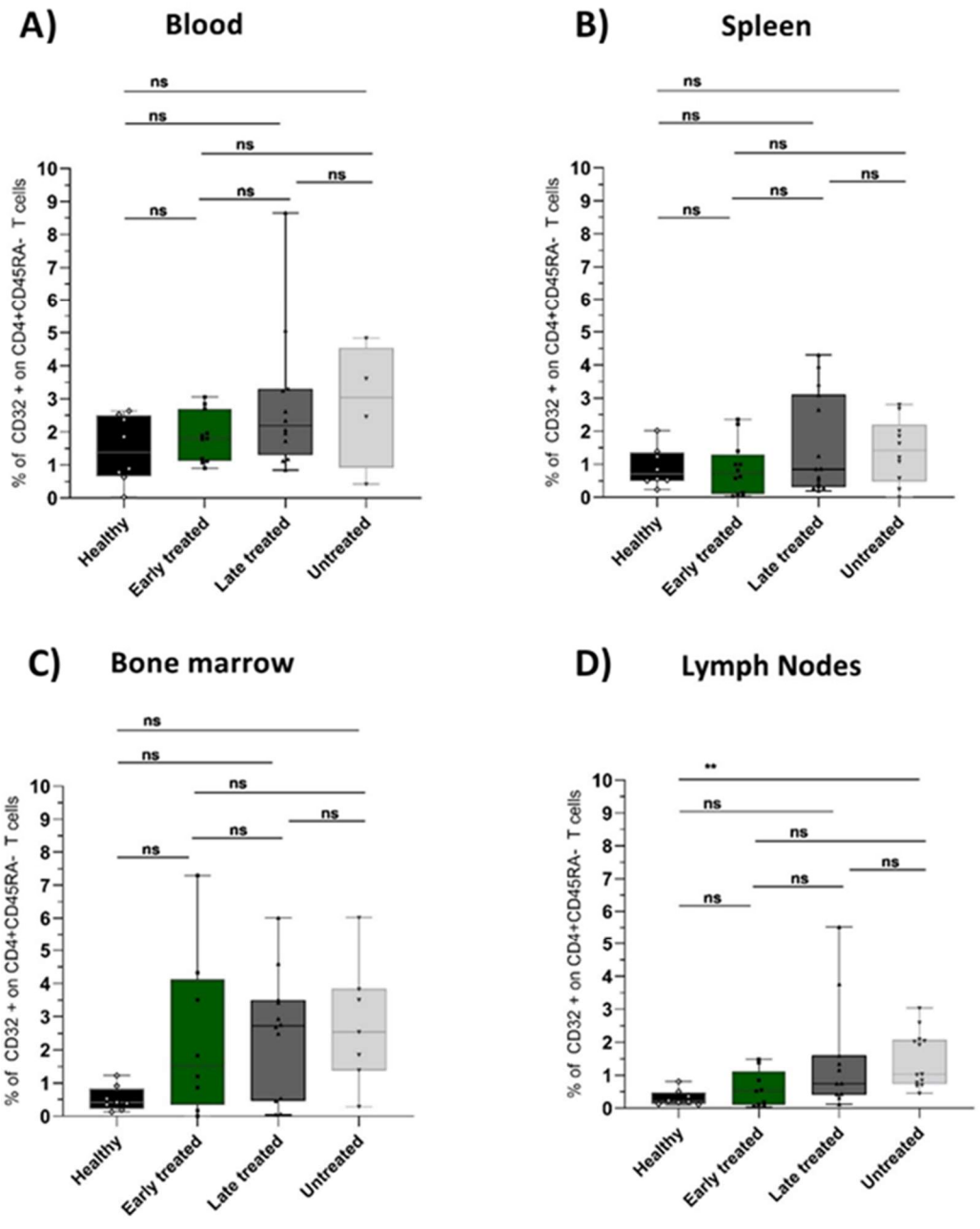

Figure S6 Related to Figure 5. CD32 expression on memory CD4$^+$ T cells from different tissues is similar between the different treatment groups

Expression of CD32 on CD4$^+$CD45RA$^-$ T cells in blood (A), spleen (B), bone marrow (C) and lymph nodes (D) from flow sorted cells of healthy uninfected mice (n=8), early treated mice (n= 8), late treated mice (n=12), and untreated mice (n= 13). Statistical testing was performed using non-parametric Kruskal Wallis test with multiple comparison Dunn's correction (**p< 0.01, ns, non significant test, p> 0.05).

Supplemental tables

Table S1 Related to Figure S6. Descriptive statistics of $CD32^{+}CD4^{+}CD45RA^{-}$ T cells from different tissues given in Figure S6 related to Figure 5.

	Groups of mice			
Tissues	Healthy	Early Treated	Late Treated	Untreated
Blood				
Number of mice	8	11	12	4
Mean	1.464	1.845	2.838	2.83
Std. Deviation	1.001	0.7517	2.172	1.876
Std. Error of Mean	0.3539	0.2266	0.6271	0.9378
Spleen				
Number of mice	8	12	15	10
Mean	0.9113	0.855	1.528	1.407
Std. Deviation	0.5946	0.7943	1.494	0.963
Std. Error of Mean	0.2102	0.2293	0.3857	0.3045
Bone marrow				
Number of mice	8	8	12	7
Mean	0.5188	2.398	2.455	2.776
Std. Deviation	0.3728	2.499	1.88	1.879
Std. Error of Mean	0.1318	0.8834	0.5426	0.7103
Lymph nodes				
Number of mice	8	9	11	13
Mean	0.315	0.5778	1.468	1.482
Std. Deviation	0.2398	0.5523	1.681	0.8409
Std. Error of Mean	0.847	0.1841	0.5068	0.2332